Accepted Preprint first posted on 13 March 2018 as Manuscript JOE-18-0086



# Uterine progesterone signaling is a target for metformin therapy in PCOS-like rats

Min Hu[1,2,†]; Yuehui Zhang[1,3,†]; Jiaxing Feng[3,†]; Xue Xu[3]; Jiao Zhang[4]; Wei Zhao[3]; Xiaozhu Guo[3]; Juan Li[1,2]; Edvin Vestin[1]; Peng Cui[1,5,6]; Xin Li[1,7,8]; Xiao-ke Wu[3]; Mats Brännström[9]; Linus R Shao[1]; and Håkan Billig[1]

[1] Department of Physiology/Endocrinology, Institute of Neuroscience and Physiology, The Sahlgrenska Academy, University of Gothenburg, 40530 Gothenburg, Sweden; [2] Department of Traditional Chinese Medicine, The First Affiliated Hospital of Guangzhou Medical University, 510120 Guangzhou, China; [3] Department of Obstetrics and Gynecology, Key Laboratory and Unit of Infertility in Chinese Medicine, First Affiliated Hospital, Heilongjiang University of Chinese Medicine, 150040 Harbin, China; [4] Department of Acupuncture and Moxibustion, Second Affiliated Hospital, Heilongjiang University of Chinese Medicine, 150040 Harbin, China; [5] Department of Integrative Medicine and Neurobiology, State Key Lab of Medical Neurobiology, Shanghai Medical College and Institute of Acupuncture Research (WHO Collaborating Center for Traditional Medicine), Institute of Brain Science, Fudan University, 200032 Shanghai, China; [6] Institute of Integrative Medicine of Fudan University, 200032 Shanghai, China; [7] Department of Gynecology, Obstetrics and Gynecology Hospital of Fudan University, 200011 Shanghai, China; [8] Shanghai Key Laboratory of Female Reproductive Endocrine Related Diseases, 200011 Shanghai, China; [9] Department of Obstetrics and Gynecology, Sahlgrenska University Hospital, Sahlgrenska Academy, University of Gothenburg, 41345 Gothenburg, Sweden

[†] The authors consider that the first three authors should be regarded as joint first authors.

*** Present address, to where correspondence and reprint requests should be addressed**

Linus R. Shao, MD, PhD., Tel: +46 31-7863408, Fax: +46 31-7863512, E-mail: linus.r.shao@fysiologi.gu.se

**Short title:** Metformin and uterine progesterone signaling

Word count of the full article, excluding references and figure legends: **4388**

Copyright © 2018 by the Society for Endocrinology.

**Abstract**

Impaired progesterone (P4) signaling is linked to endometrial dysfunction and infertility in women with polycystic ovary syndrome (PCOS). Here we report for the first time that elevated expression of progesterone receptor (PGR) isoforms A and B parallels increased estrogen receptor (ER) expression in PCOS-like rat uteri. The aberrant PGR-targeted gene expression in PCOS-like rats before and after implantation overlaps with dysregulated expression of *Fkbp52* and *Ncoa2*, two genes that contribute to the development of uterine P4 resistance. *In vivo* and *in vitro* studies of the effects of metformin on the regulation of the uterine P4 signaling pathway under PCOS conditions showed that metformin directly inhibits the expression of PGR and ER along with the regulation of several genes that are targeted dependently or independently of PGR-mediated uterine implantation. Functionally, metformin treatment corrected the abnormal expression of cell-specific PGR and ER and some PGR-target genes in PCOS-like rats with implantation. Additionally, we documented how metformin contributes to the regulation of the PGR-associated MAPK/ERK/p38 signaling pathway in the PCOS-like rat uterus. Our data provide novel insights into how metformin therapy regulates uterine P4 signaling molecules under PCOS conditions.

**Key words:** Metformin, progesterone receptor, MAPK/ERK/p38 signaling pathway, implantation, polycystic ovary syndrome

51 **Introduction**

52 Polycystic ovary syndrome (PCOS) is a clinically and etiologically heterogeneous
53 hormone-imbalance disorder that is associated with multiple reproductive and metabolic
54 abnormalities (Rosenfield and Ehrmann 2016). Women suffering from PCOS present with
55 arrested folliculogenesis and chronic anovulation-linked infertility (Azziz *et al.* 2016;
56 Rosenfield and Ehrmann 2016), and they also have more adverse reproductive risk as
57 evidenced by an increase in the prevalence of implantation failure, recurrent miscarriage,
58 spontaneous abortion, premature delivery, endometrial carcinoma (Goodarzi *et al.* 2011;
59 Palomba *et al.* 2015; Shao *et al.* 2014b). In addition to the ovarian dysfunction (Azziz *et al.*
60 2016; Rosenfield and Ehrmann 2016), it is assumed that the impairment of endometrial
61 function also contributes to PCOS-associated infertility (Evans *et al.* 2016). Although
62 progesterone (P4)-based oral contraceptive therapy is often efficacious (Lopes *et al.* 2014;
63 Vrbikova and Cibula 2005), perturbations in endometrial P4 signaling that result from
64 attenuated responsiveness and resistance to P4 are common in the endometrium of a PCOS
65 patient (Li *et al.* 2014a; Piltonen 2016). P4 resistance is a condition in which tissues and cells
66 do not respond appropriately to P4 (Chrousos *et al.* 1986), and this is evidenced by
67 endometriosis and endometrial hyperplasia that may progress to endometrial carcinoma
68 despite supplementation with P4 or its analogs (Gunderson *et al.* 2012; Shao *et al.* 2014a).
69 Gene profiling experiments have shown that different endometrial genes are likely to act in
70 concert in this abnormal condition in PCOS patients (Kim *et al.* 2009; Savaris *et al.* 2011);
71 however, how changes in the expression of P4 signaling molecules contribute to the P4
72 resistance in a PCOS patient's endometrium is poorly understood.

73 P4 is an essential contributing factor in female reproductive tissues that regulates multiple
74 physiological processes such as the menstrual cycle, implantation, pregnancy maintenance,
75 and labor initiation (Evans *et al.* 2016). There are two major progesterone receptor (PGR)

76 isoforms, PGRA and PGRB, both of which are involved in a common P4 signaling pathway
77 for uterine cell-specific proliferation and differentiation (Li *et al.* 2014a; Patel *et al.* 2015). P4
78 binding activates both PGR isoforms and leads to translocation from the cytosol to the
79 nucleus followed by binding to the P4-responsive elements of the target genes, resulting in
80 alterations of PGR-targeted gene expression depending on the recruitment of co-regulators
81 (Patel *et al.* 2015). It has been reported that endometrial PGR expression is elevated in PCOS
82 patients who have anovulation compared to PCOS patients who still ovulate and to non-PCOS
83 patients (Margarit *et al.* 2010; Quezada *et al.* 2006). Additionally, PGR activity is also
84 modulated by the cytoplasmic mitogen-activated protein kinase (MAPK)/extracellular signal-
85 regulated kinase (ERK) signaling pathway (Gellersen and Brosens 2014; Patel *et al.* 2015).
86 While high levels of ERK1/2 expression and activation reflect the P4-PGR signaling-induced
87 decidualization status in human and rodent uteri (Lee *et al.* 2013; Tapia-Pizarro *et al.* 2017;
88 Thienel *et al.* 2002), it remains to be determined whether suppression of MAPK/ERK
89 signaling occurs in the endometrium and whether such dysregulation can negatively impact
90 uterine function under PCOS conditions.

91 Metformin is an anti-diabetic drug that is a clinically approved treatment in PCOS patients
92 worldwide (Naderpoor *et al.* 2015). Several diverse molecular mechanisms of metformin have
93 been demonstrated in human endometrial carcinoma tissues *in vivo* and in different
94 endometrial cancer cells *in vitro* (Shao *et al.* 2014b), and metformin's therapeutic effects on
95 endometrial function are evidenced by improvement of endometrial receptivity, enhancement
96 of endometrial vascularity and blood flow, and reversion of endometrial hyperplasia and
97 carcinoma into normal endometria in some women with PCOS (Jakubowicz *et al.* 2001; Li *et*
98 *al.* 2014b; Palomba *et al.* 2006). Our recent studies using a PCOS-like rat model found that
99 chronic treatment with metformin has significant anti-androgenic and anti-inflammatory
100 impacts in the uterus (Zhang *et al.* 2017). Given the central role of P4 signaling in uterine

101 implantation (Evans *et al.* 2016; Patel *et al.* 2015) and the ability of metformin to rescue
102 implantation failure in some PCOS-like rats by modulating the expression of multiple
103 implantation-related genes in the uterus *in vivo* (Zhang *et al.* 2017), we speculated that the
104 beneficial effects of metformin might be mechanistically linked to the uterine P4 signaling
105 pathway under pathological conditions such as PCOS. To address this hypothesis, we
106 analyzed PCOS-associated PGR isoform expression and the MAPK signaling network in
107 human and rat uterine tissues. By combining a PCOS-like rat model (Zhang *et al.* 2016) and
108 *in vitro* tissue culture approach (Li *et al.* 2015), we aimed to determine whether metformin
109 directly reverses aberrant PGR-targeted and implantation-related gene expression in the
110 PCOS-like rat uterus.

111 **Materials and Methods**

112 ***Study approval***

113 All animal experiments were performed according to the National Institutes of Health
114 guidelines on the care and use of animals and were approved and authorized by the Animal
115 Care and Use Committee of the Heilongjiang University of Chinese Medicine, China (HUCM
116 2015-0112).

117 ***Experimental animals and tissue preparations***

118 Adult female Sprague–Dawley rats (n = 134) were obtained from the Laboratory Animal
119 Centre of Harbin Medical University, Harbin, China (License number SCXK 2013-001).
120 Animals were housed in the animal care facility with free access to food and water and a
121 controlled temperature of 22°C ± 2°C with a 12 h light/dark cycle. Estrous cycles were
122 monitored daily by vaginal lavage according to a standard protocol (Feng *et al.* 2010). All rats
123 (70 days old) with the different stages of estrous cycle used in this study were confirmed by
124 examination of vaginal smears under a light microscope for two sequential cycles (about 8–10

125 days). Any PCOS-like (insulin+hCG-treated) rats that exhibited prolonged estrous cycles
126 (more than 5 days) were excluded from the study.

127 Experiment 1: Rats were randomly divided into control (saline treatment, n = 20) and
128 experimental (PCOS-like, n = 20) groups. The experimental group was treated with insulin
129 plus hCG to induce a PCOS-like metabolic and reproductive phenotype, and the control rats
130 were treated with an equal volume of saline (Zhang *et al.* 2018; Zhang *et al.* 2016). In brief,
131 insulin was started at 0.5 IU/day and gradually increased to 6.0 IU/day between day 1 and the
132 day 22 to induce hyperinsulinemia and insulin resistance, and 3.0 IU/day hCG was given on
133 all 22 days to induce hyperandrogenism. Animals were treated with twice-daily subcutaneous
134 injections until the end of the experiment. Rats with repeated insulin injections have not
135 shown any hypoglycemic episodes (Bogovich *et al.* 1999; Damario *et al.* 2000; Poretsky *et al.*
136 1992; Zhang *et al.* 2018). Detailed analysis of endocrine and metabolic parameters as well as
137 the uterine morphology in these animals has been reported previously (Zhang *et al.* 2016). On
138 day 23, each group of rats was divided into two subgroups of 10 rats each (Supplemental Fig.
139 1A). For treatment, metformin was dissolved in saline and given as a daily oral dose of 500
140 mg/kg by a cannula. The treatment time and tissue collection are described in our previous
141 study (Zhang *et al.* 2017).

142 Experiment 2: Rats were randomly divided into control (saline treatment, n = 21) and
143 experimental (PCOS-like, n = 15) groups and treated as described in Experiment 1
144 (Supplemental Fig. 1B). After metformin treatment, control and PCOS-like rats were mated
145 with fertile males of the same strain to induce implantation, which was determined by the
146 presence of a vaginal plug (day 1 of pregnancy). The rats were sacrificed between 0800 and
147 0900 hours on day 6 of pregnancy. To identify the implantation sites, rats were injected
148 intravenously with a Chicago Blue B dye solution (1% in saline) and sacrificed 10 min later.

149 Uteri were dissected and assessed for clearly delineated blue bands as evidence of early
150 implantation sites as described previously (Zhang *et al.* 2017).

151 Experiment 3: Rats were divided into control (saline treatment, n = 9) and experimental
152 (PCOS-like, n = 39) groups and treated as described in the Experiment 1. On the 23rd day, the
153 PCOS-like rats were divided into four subgroups and treated daily with P4 (4 mg/kg), RU486
154 (6 mg/kg), or both for 3 days. For treatment, P4 and RU486 were dissolved in 100% ethanol
155 and resuspended in sesame oil. All subcutaneous injections were in a volume of 100 μl. An
156 equal volume of 100% ethanol and sesame oil was injected into both healthy control rats and
157 PCOS-like rats as experimental controls (Supplemental Fig. 1C). The pharmacological doses
158 and treatment time intervals of P4 and RU486 were chosen on the basis of previous studies
159 (Kim *et al.* 2006; Knox *et al.* 1996).

160 After dissection, the uterine horns were trimmed free of fat and connective tissue. One side
161 of the uterus in each animal was fixed in 10% neutral formalin solution for 24 h at 4ºC and
162 embedded in paraffin for histochemical analysis. The other side was immediately frozen in
163 liquid nitrogen and stored at −70ºC for Western blot and quantitative real-time PCR (qRT-
164 PCR) analysis.

165 Detailed description of the methods including the primary *in vitro* tissue culture and
166 treatment, morphological assessment and immunostaining, protein isolation and Western blot
167 analysis, RNA extraction and qRT-PCR analysis, and measurement of biochemical
168 parameters used in this study are provided in Supplemental files.

169 ***Statistical analysis***

170 GraphPad Prism was used for statistical analysis and graphing. For all experiments, n-
171 values represent the number of individual animals. Data are represented as the means ± SEM.
172 Statistical analyses were performed using SPSS version 24.0 statistical software for Windows
173 (SPSS Inc., Chicago, IL). The normal distribution of the data was tested with the Shapiro–

174 Wilk test. Differences between groups were analyzed by one-way ANOVA or two-way
175 ANOVA, and this was followed by Tukey's post-hoc test for normally distributed data or the
176 Kruskal–Wallis test followed by the Mann–Whitney U-test for skewed data. All *p*-values less
177 than 0.05 were considered statistically significant.

178 **Results**

179 ***Metformin alters PGR isoform and PGR-targeted gene expression in PCOS-like rats***

180 The insulin+hCG-treated rats exhibit reproductive disturbances that mimic human PCOS
181 (Zhang *et al.* 2017; Zhang *et al.* 2016). Prompted by these findings, we set out to investigate
182 the impact of P4 signaling in this model. First, we showed that although the ratio of PGRA to
183 PGRB was not significantly different between control and PCOS-like rats, the PCOS-like rats
184 had increased levels of uterine PGRA and PGRB (Fig. 1A). While PGR immunoreactivity
185 was primarily evidenced in control rat uterine luminal and glandular epithelia as well as in the
186 stroma, the immunoreactivity of luminal epithelial PGR expression was associated with
187 increased numbers of luminal epithelial cells and increased immunoreactivity of PGR in the
188 stroma in PCOS-like rats (Fig. 1B). Metformin treatment did not significantly affect PGR
189 isoform expression in control rats and PCOS-like rats compared to those rats treated with
190 saline (Fig. 1A). However, we found that PGR immunoreactivity was decreased in the
191 luminal and glandular epithelia by metformin treatment in both control rats and PCOS-like
192 rats compared to those treated with saline (Fig. 1B). Conversely, intense immunoreactivity of
193 PGR expression was detected in the stroma located close to the luminal epithelia in control
194 and PCOS-like rats treated with metformin (Fig. 1B). In contrast to the epithelia and stroma,
195 no significant changes in PGR expression in the myometrium were found in any of the groups
196 (data not shown). Because a large body of evidence indicates that regulation of P4 signaling
197 results in changes in the expression of several PGR-targeted genes in the uterus (Bhurke *et al.*
198 2016), we profiled the expression of genes that are indicators for PGR activity in the rat uterus

199 by qRT-PCR. Quantitative data indicated that *Smo*, and *Nr2f2* mRNA levels were increased in
200 PCOS-like rats compared to control rats treated with saline. In contrast, the *Fkbp52* mRNA
201 level was decreased in PCOS-like rats compared to control rats (Fig. 1C). We next determined
202 the actions of metformin treatment on PGR-targeted gene expression and showed that *Ptch*,
203 *Fkbp52*, and *Ncoa2* levels were increased in PCOS-like rats treated with metformin compared
204 to PCOS-like rats treated with saline, while *Smo* and *Nr2f2* mRNA levels were decreased on
205 PCOS-like rats treated with metformin compared to those treated with saline (Fig. 1C).

206 ***Metformin partially prevents implantation failure in parallel with regulation of PGR***
207 ***isoform and PGR-targeted gene expression in PCOS-like rats***

208 Metformin has been shown to partially rescue the disruption of the implantation process in
209 PCOS-like rats (Zhang *et al.* 2017), and the altered endocrine and metabolic parameters in
210 these animals are shown in Supplemental Table 4. After metformin treatment, total
211 testosterone levels, the ratio of total testosterone to androstenedione, and fasting insulin levels
212 were all significantly higher in PCOS-like rats where implantation did not occur compared to
213 those with implantation, as was insulin resistance as assessed by the homeostasis model
214 assessment of insulin resistance, mirroring the endocrine and metabolic abnormalities in
215 PCOS patients (Azziz *et al.* 2016; Rosenfield and Ehrmann 2016). Of note, PCOS-like rats
216 that failed to implant embryos also exhibited decreased P4 levels. These data suggest that
217 implantation failure in PCOS-like rats treated with metformin is due not only to
218 hyperandrogenism and insulin resistance, but also to impairment of P4 signaling in the uterus.
219 Further morphological characterization of metformin-treated PCOS-like rats with no
220 implantation revealed the infiltration of immune cells into the glandular epithelial cell layer in
221 a similar manner to when hormone imbalances were studied in a previous report (Wira *et al.*
222 2005) (Supplemental Fig. 3, black arrowheads). To determine how impairment of P4
223 signaling causes implantation failure, we subsequently analyzed PGR isoform and PGR-

224 targeted gene expression in PCOS-like rats with no implantation. Although treatment with
225 metformin increased PGR isoform expression in control and PCOS-like rats, neither the
226 PGRA nor PGRB protein level was altered between PCOS-like rats with implantation and
227 with failed implantation (Fig. 2A). As shown in Figure 2B, while PGR protein was expressed
228 in the decidualizing stroma at the site of implantation in all groups, PGR immunoreactivity
229 was increased in the stroma of the inter-implantation region in control rats treated with
230 metformin. Furthermore, we found that the immunoreactivity of PGR was increased in the
231 epithelia in PCOS-like rats without implantation despite metformin treatment. Thus,
232 metformin appeared to participate in the regulation of uterine PGR expression in a cell type-
233 specific manner in PCOS-like rats before and after implantation. qRT-PCR data indicated that
234 *Ihh* and *Ncoa2* mRNAs were increased and that *Ptch* and *Fkbp52* mRNAs were decreased in
235 metformin-treated PCOS-like rats with no implantation compared to control rats treated with
236 saline or metformin and to metformin-treated PCOS-like rats with implantation (Fig. 2C).

237 ***Metformin directly regulates PGR isoform, PGR-target, and implantation-related gene***
238 ***expression in vitro***

239 Based on these *in vivo* observations, we asked whether the effect of metformin was direct
240 or indirect in the PCOS-like rat uterus. *In vitro* uterine tissue culture experiments revealed that
241 *Pgr* and *Pgrb*, mRNA levels were higher in PCOS-like rats compared to control rats, in
242 agreement with alteration of PGR isoform protein expression (Fig. 1C). Furthermore,
243 metformin treatment increased *Pgr* and *Pgrb* mRNA levels in control and PCOS-like rats in a
244 time-dependent manner (Fig. 3A). Consistent with the *in vivo* effects of metformin in PCOS-
245 like rats (Fig. 1C), *Ihh*, *Smo*, and *Nr2f2* mRNA levels were increased in the PCOS-like rat
246 uterus compared to the control rat uterus and were down-regulated by metformin treatment *in*
247 *vitro*. While the *Hand2* mRNA level was upregulated by metformin treatment at 48 h and 72 h,

248 we detected the upregulation of *Ptch*, *Fkbp52*, and *Ncoa2* mRNA levels in the PCOS-like rat
249 uterine tissues over a 72-h course after metformin treatment (Fig. 3A).

250 The expression of a number of implantation-related genes has been reported to be
251 regulated by metformin treatment in PCOS-like rats during implantation (Zhang *et al.* 2017).
252 These previous observations prompted further analysis of implantation-related gene
253 expression by metformin treatment *in vitro*. In contrast to the different regulation patterns of
254 *Spp1*, *Lrh1*, *Sgk1*, and *Krt13* mRNAs under *in vivo* and *in vitro* conditions, the *in vitro*
255 responses of uterine *Prl*, *Igfbp1*, *Il11*, *Pc6*, *Maoa*, *Ednrb*, *Hoxa10*, *Hoxa11*, and *Hbegf* mRNA
256 levels to metformin (Fig. 3B) were coincident with the *in vivo* regulation of the expression
257 pattern of these genes (Zhang *et al.* 2017). Our data indicated that metformin directly up-
258 regulates uterine *Prl*, *Maoa*, *Ednrb*, and *Hbegf* mRNA levels in PCOS-like rats during
259 implantation *in vivo*.

260 To ascertain whether the modulation of uterine gene expression is P4-mediated and PGR-
261 dependent in PCOS-like rats, insulin+hCG-treated rats were injected subcutaneously with P4
262 and/or RU 486 for three days. As shown in Figure 4, the increased PGR isoform protein levels
263 (Fig. 1A) were confirmed by analysis of *Pgr* and *Pgrb* mRNA expression in the PCOS-like
264 rat uterus. Although treatment with P4 and/or RU486 did not significantly affect *Pgr* mRNA
265 expression, we found that *Pgrb* mRNA levels were decreased in PCOS-like rats compared to
266 those rats with no treatment (Fig. 4). Among seven PGR-targeted genes (Fig. 1C), we found
267 that *Ptch*, *Hand2*, and *Fkbp52* mRNA levels were increased and that *Ihh*, *Smo*, and *Nr2f2*
268 mRNA levels were decreased in PCOS-like rats treated with P4 compared to those rats with
269 no treatment. We also observed that treatment with RU486 alone or combined with P4
270 reversed the changes in *Smo*, *Hand2*, and *Fkbp52* mRNA levels in PCOS-like rats (Fig. 4). No
271 significant differences of uterine *Ncoa2* mRNA expression were observed in PCOS-like rats
272 regarding the different treatments. Based on our current experimental approaches, it is likely

273 that another regulatory mechanism contributes to the metformin-induced up-regulation of
274 *Ncoa2* mRNA levels in PCOS-like rats.

275 ***Metformin regulates the MAPK signaling pathway in PCOS-like rats before and after***
276 ***implantation***

277 In an attempt to understand the changes in PGR activation and function observed in PCOS
278 patients (Patel *et al.* 2015), we performed a Western blot analysis to measure the expression
279 of several proteins that are involved in the MAPK signaling pathway in the uterus after
280 metformin treatment. As shown in Figure 5A, there was no significant difference in p-c-Raf,
281 p-MEK1/2, p-ERK1/2, p-p38 MAPK, or p38 MAPK expression between saline-treated and
282 metformin-treated rats. Quantitative protein data indicated that the expression of p-p38
283 MAPK and p38 MAPK was significantly decreased in PCOS-like rats compared to control
284 rats. Nevertheless, metformin treatment only reversed p-p38 MAPK protein expression in
285 PCOS-like rats.

286 We next assessed whether the MAPK/ERK signaling pathway contributes to uterine
287 implantation in control and PCOS-like rats treated with metformin. As shown in Figure 5B,
288 although the p-MEK1/2 level was decreased in control rats treated with metformin compared
289 to control rats treated with saline, no significant difference in p-c-Raf, p-ERK1/2, ERK1/2, p-
290 p38 MAPK, or p38 MAPK expression between these two groups was found. Furthermore, our
291 data showed that p-c-Raf, p-MEK1/2, and p-ERK1/2 protein levels were down-regulated in
292 PCOS-like rats treated with metformin regardless of the occurrence of implantation. We also
293 found that after metformin treatment PCOS-like rats with implantation exhibited decreased p-
294 p38 MAPK, but not p38 MAPK, expression.

295 ***Up-regulation of estrogen receptor (ER) expression in PCOS-like rats can be suppressed by***
296 ***metformin***

297 Because estrogen-ER signaling regulates uterine PGR expression and activity (Li *et al.*
298 2014a; Patel *et al.* 2015) and because increased circulating E2 in PCOS-like rats can be
299 inhibited by metformin treatment (Zhang *et al.* 2017), we sought to determine whether ER
300 subtypes (ERα and ERβ) are involved in the regulation of aberrant PGR expression in PCOS-
301 like rats and, if so, if metformin possibly alters ER subtype expression. Our data showed that
302 PCOS-like rats exhibited increased *Esr1* (ERα) and *Esr2* (ERβ) mRNA levels, which were
303 suppressed by metformin treatment. As shown in Figure 6A, while nuclear ERα
304 immunoreactivity was detected in the epithelia and stroma in control rats treated with saline
305 (Fig. 6B1), immunoreactivity of ERα was increased in the glandular epithelia and stroma in
306 PCOS-like rats (Fig. 6D1). Furthermore, treatment with metformin led to decreased ERα
307 immunoreactivity in control (Fig. 6C1) and PCOS-like rats (Fig. 6E1). No obvious difference
308 in ERα immunoreactivity was observed in the myometrium in any of the groups (Fig. 6B2-
309 E2). We also found that ERβ was mainly co-localized with ERα in the epithelia and stroma
310 but not in the myometrium in control and PCOS-like rats regardless of the different
311 treatments. Furthermore, with metformin treatment, we noted a significant increase in uterine
312 *Esr1* and *Esr2* mRNAs in PCOS-like rats without implantation (Fig. 7A).
313 Immunofluorescence staining revealed that, overall, immunoreactivities of both ERα and ERβ
314 were diminished in the decidualizing stroma at the site of implantation (Fig. 7B1–D1), in the
315 epithelia and stroma of the inter-implantation region (Fig. 7B2–D2) in control rats treated
316 with saline or metformin (Fig. 7B2–C2), and in the inter-implantation site of PCOS-like rats
317 treated with metformin (Fig. 7D2) compared to those rats before implantation (Fig 6. B1–E2).
318 Interestingly, PCOS-like rats with no implantation exhibited sustained nuclear ERα
319 immunoreactivity in the glandular epithelia and stroma (Fig. 7E1).

320 ***Differential cell-specific expression of phospho-histone H3 in PCOS-like rats treated with***
321 ***metformin***

322 As previously demonstrated (Avellaira *et al.* 2006), p-histone H3 is of special interest
323 because the endometrium of PCOS patients displays high levels of p-histone H3, which is
324 associated with cellular processes such as mitosis (Brenner *et al.* 2003). Quantitative
325 assessment of p-histone H3 indicated that no significant change in p-histone H3
326 immunoreactivity was present in the epithelia or stroma in any of groups (Supplemental Fig.
327 4E); however, metformin treatment decreased p-histone H3 immunoreactivity in the
328 myometrium in PCOS-like rats compared to those treated with saline. Of note, intensely p-
329 histone H3-positive stromal cells close to the luminal and glandular epithelia were found in
330 PCOS-like rats treated with metformin (Supplemental Fig. 4D2). Similarly, p-histone H3
331 immunoreactivity was significantly increased in the stroma at the inter-implantation sites in
332 PCOS-like rats treated with metformin independently of implantation (Supplemental Fig. 5E).
333 In PCOS-like rats without implantation, p-histone H3 immunoreactivity was often detected in
334 the luminal epithelia (Supplemental Fig. 5D1), although this was not statistically significant
335 compared to PCOS-like rats with implantation (Supplemental Fig. 5E). It is thus likely that
336 the regulation of mitotic activity by metformin is cell type-dependent in the uterus.

337 **Discussion**

338 Reproductive dysfunction and infertility manifest noticeably in PCOS patients (Evans *et al.*
339 2016). In striking contrast to the attention given to hyperandrogenism and insulin resistance in
340 women with PCOS, the aberrant P4 signaling pathway resulting in uterine P4 resistance has
341 received much less attention (Li *et al.* 2014a; Piltonen 2016). This study is the first to show
342 that the therapeutic effects of metformin on the regulation of uterine function in PCOS-like
343 rats is mediated through P4 signaling.

344 Elucidating the regulation of endometrial PGR levels under PCOS conditions is important
345 clinically. Our data show that increased PGR expression is paralleled with elevated ER
346 expression in PCOS-like rats. This expression pattern is associated with an increased

347 circulating E2 level (Zhang *et al.* 2016), suggests that E2-ER signaling contributes to the up-
348 regulation of PGR under PCOS conditions *in vivo*. Similar to PCOS patients (Hu *et al.*
349 submitted), PCOS-like rats also displayed high levels of PGR isoforms and ER subtypes in
350 the uterus. The induction of implantation is required for the activation of PGR, and
351 implantation subsequently alters gene expression in the endometrium (Gellersen and Brosens
352 2014; Patel *et al.* 2015); however, PGR-targeted gene expression in PCOS patients and
353 PCOS-like rats has only been demonstrated to a limited degree. The current study shows that
354 significantly decreased *Fkbp52* gene expression parallels increased expression of *Ihh*, *Smo*,
355 and *Nr2f2* mRNAs without changes in *Ncoa2* mRNA in PCOS-like rats. In addition, we also
356 found that abnormal expression of PGR-target genes, including *Fkbp52* and *Ncoa2*, is
357 retained in PCOS-like rats with implantation failure. This is supported by *in vivo* studies
358 showing that mice lacking *Fkbp52* (Tranguch *et al.* 2007; Yang *et al.* 2006) or *Ncoa2*
359 (Mukherjee *et al.* 2007; Mukherjee *et al.* 2006) demonstrate the absence of decidualization
360 after P4 supplementation due to diminished P4 responsiveness. Previous studies have reported
361 that women with endometriosis and endometrial hyperplasia/carcinoma who develop P4
362 resistance have low levels of PGR expression (Gunderson *et al.* 2012; Shao *et al.* 2014a).
363 Although it is currently unclear why differences exist in the regulation of uterine PGR
364 expression between different diseases with P4 resistance, it is likely that uterine P4 resistance
365 in PCOS-like rats is due to impaired PGR activity rather than PGR expression.

366 Defects in PGR isoform-specific P4 signaling in the mouse uterus can give rise to distinct
367 phenotypes of uterine impairment and implantation failure (Li *et al.* 2014a). Here we
368 observed no changes in total *Pgr* mRNA levels but a reduction of *Pgrb* mRNA levels in
369 PCOS-like rat uterus after treatment with P4 and/or RU486. This suggests that uterine *Pgra*
370 mRNA levels are increased. Meanwhile, several PGR target genes (e.g., *Ihh*, *Smo*, *Ptch*,
371 *Nr2f2*, *Hand2*, and *Fkbp52*) are significantly altered in PCOS-like rats after P4 treatment.

372 Thus, we speculate that changes in these P4-dependnent PGR target gene expression in
373 PCOS-like rat uterus might be accounted for by an increase in *Pgra* mRNA expression.
374 Studies of mutant mice lacking specific PGR isoform will clarify the functional differences
375 between the two PGR isoforms in the progression of PCOS-induced uterine dysfunction.

376 P4-mediated and PGR-dependent regulation of ERK1/2 expression plays a critical role in
377 humans and rodents during endometrial decidualization and implantation (Lee *et al.* 2013;
378 Tapia-Pizarro *et al.* 2017; Thienel *et al.* 2002), but such regulation under PCOS conditions
379 has not previously been reported. The inhibition of ERK1/2 expression and activation has
380 been reported in ovarian granulosa and thecal cells in PCOS patients (Lan *et al.* 2015; Nelson-
381 Degrave *et al.* 2005), and we have previously shown that the expression and activation of
382 uterine ERK1/2 is suppressed in rats treated with insulin and hCG to induce the PCOS
383 phenotype (Zhang *et al.* 2016). The present study supports and extends this work. Here we
384 observed no changes in p-ERK1/2 or ERK1/2 expression in the rat uterus after prolonged
385 treatment with insulin and hCG. However, we observed that the levels of p-c-Raf and p-
386 MEK1/2, two upstream regulators of ERK1/2, were significantly decreased in PCOS-like rats
387 after uterine implantation, establishing a tight link between different MAPK/ERK signaling
388 molecules. Our data suggest that regulation of uterine ERK1/2 expression *in vivo* is time-
389 dependent (Lee *et al.* 2013; Tapia-Pizarro *et al.* 2017; Thienel *et al.* 2002), which is similar to
390 the regulation of PGR isoforms and PGR-targeted gene expression. The MAPK/ERK/p38
391 signaling pathway contributes to the regulation of inflammation and cytokine production
392 (Arthur and Ley 2013; Cuadrado and Nebreda 2010), and the dysregulation of inflammation-
393 related molecules is associated with PCOS conditions (Matteo *et al.* 2010; Orostica *et al.*
394 2016; Piltonen *et al.* 2013; Piltonen *et al.* 2015). Furthermore, like the activation of NFκB
395 signaling that induces the transcriptional levels of inflammation-related gene expression in
396 ovarian granulosa cells and in serum in PCOS patients (Liu *et al.* 2015; Zhao *et al.* 2015), our

397 previous study has shown that the sustained metformin treatment markedly suppresses uterine
398 inflammatory gene expression, especially the *Il-6* and *TNFα* mRNAs that are associated with
399 inhibition of nuclear NFκB translocation in PCOS-like rats (Zhang *et al.* 2017). Importantly,
400 p38 can antagonize ERK1/2 signaling mediated by protein phosphatase 2A and consequently
401 down-regulate inflammatory cytokine and chemokine production (Cuadrado and Nebreda
402 2010), and the anti-inflammatory effects of MAPK/p38 are involved in the regulation of
403 NFκB activity (Arthur and Ley 2013). These observations further indicate that metformin
404 inhibits NFκB-driven inflammatory processes through p38 activation rather than through
405 ERK1/2 inhibition in the PCOS-like rat uterus.

406 The results of the present study permit us to draw the following conclusions (Figure 8). 1)
407 With sustained low levels of P4, the expressions of both uterine PGR isoforms are elevated in
408 PCOS-like rats *in vivo*. This is positively associated with the high levels of ERs in PCOS-like
409 rats. Consistent with mouse knockout studies, altered expression of *Fkbp52* and *Ncoa2*, two
410 genes that contribute to uterine P4 resistance, is seen in PCOS-like rats before and after
411 implantation. 2) Metformin directly suppresses uterine PGR isoform expression along with
412 the correction of aberrant expression of PGR-targeted and implantation-related genes in
413 PCOS-like rats. Abnormal cell-specific regulation of PGR and ER, paralleling the aberrant
414 expression of PGR-targeted and implantation-related genes, is retained in PCOS-like rats with
415 implantation failure. 3) Increased PGR expression is associated with inhibition of the
416 MAPK/ERK/p38 signaling pathway, and the primary effect of metformin treatment is to
417 restore the MAPK/p38 signaling pathway in the PCOS-like rat uterus. Taken together, our
418 findings provide support for metformin therapy in the improvement of P4 signaling in PCOS-
419 like rats with uterine dysfunction and for its clinical relevance in the treatment of PCOS
420 patients with P4 resistance.

421

422 **Declaration of interest**

423 The authors declare that there is no conflict of interest that could be perceived as prejudicing
424 the impartiality of the research reported.

425 **Funding**

426 Research reported in this publication was supported by the Swedish Medical Research
427 Council (grant number 10380), the Swedish federal government under the LUA/ALF
428 agreement (grant number ALFGBG-147791), the Jane and Dan Olsson's Foundation, the
429 Hjalmar Svensson Foundation, and the Adlerbert Research Foundation (to HB and LRS) as
430 well as the National Natural Science Foundation of China (grant number 81774136), the
431 Project of Young Innovation Talents in Heilongjiang Provincial University (grant number
432 UNPYSCT-2015121), the Project of Innovation Talents (Young Reserve Talents) in Harbin
433 city (grant number 2015RAQYJ089), and the Project of Excellent Innovation Talents by
434 Heilongjiang University of Chinese Medicine (to YZ).

435 **Acknowledgements**

436 The authors thank the Centre for Cellular Imaging at the University of Gothenburg and the
437 National Microscopy Infrastructure (grant number VR-RFI 2016-00968) for providing
438 assistance in microscopy.

439

440 **REFERENCES**

441 Arthur JS & Ley SC 2013 Mitogen-activated protein kinases in innate immunity. *Nat Rev*
442 *Immunol* **13** 679-692.
443 Avellaira C, Villavicencio A, Bacallao K, Gabler F, Wells P, Romero C & Vega M 2006
444 Expression of molecules associated with tissue homeostasis in secretory endometria from
445 untreated women with polycystic ovary syndrome. *Hum Reprod* **21** 3116-3121.
446 Azziz R, Carmina E, Chen Z, Dunaif A, Laven JS, Legro RS, Lizneva D, Natterson-Horowtiz
447 B, Teede HJ & Yildiz BO 2016 Polycystic ovary syndrome. *Nat Rev Dis Primers* **2** 16057.
448 Bhurke AS, Bagchi IC & Bagchi MK 2016 Progesterone-Regulated Endometrial Factors
449 Controlling Implantation. *Am J Reprod Immunol* **75** 237-245.
450 Bogovich K, Clemons J & Poretsky L 1999 Insulin has a biphasic effect on the ability of
451 human chorionic gonadotropin to induce ovarian cysts in the rat. *Metabolism* **48** 995-1002.
452 Brenner RM, Slayden OD, Rodgers WH, Critchley HO, Carroll R, Nie XJ & Mah K 2003
453 Immunocytochemical assessment of mitotic activity with an antibody to phosphorylated
454 histone H3 in the macaque and human endometrium. *Hum Reprod* **18** 1185-1193.
455 Chrousos GP, MacLusky NJ, Brandon DD, Tomita M, Renquist DM, Loriaux DL & Lipsett
456 MB 1986 Progesterone resistance. *Adv Exp Med Biol* **196** 317-328.
457 Cuadrado A & Nebreda AR 2010 Mechanisms and functions of p38 MAPK signalling.
458 *Biochem J* **429** 403-417.
459 Damario MA, Bogovich K, Liu HC, Rosenwaks Z & Poretsky L 2000 Synergistic effects of
460 insulin-like growth factor-I and human chorionic gonadotropin in the rat ovary. *Metabolism*
461 **49** 314-320.
462 Evans J, Salamonsen LA, Winship A, Menkhorst E, Nie G, Gargett CE & Dimitriadis E 2016
463 Fertile ground: human endometrial programming and lessons in health and disease. *Nat Rev*
464 *Endocrinol* **12** 654-667.
465 Feng Y, Weijdegard B, Wang T, Egecioglu E, Fernandez-Rodriguez J, Huhtaniemi I, Stener-
466 Victorin E, Billig H & Shao R 2010 Spatiotemporal expression of androgen receptors in the
467 female rat brain during the oestrous cycle and the impact of exogenous androgen
468 administration: a comparison with gonadally intact males. *Mol Cell Endocrinol* **321** 161-174.
469 Gellersen B & Brosens JJ 2014 Cyclic decidualization of the human endometrium in
470 reproductive health and failure. *Endocr Rev* **35** 851-905.
471 Goodarzi MO, Dumesic DA, Chazenbalk G & Azziz R 2011 Polycystic ovary syndrome:
472 etiology, pathogenesis and diagnosis. *Nat Rev Endocrinol* **7** 219-231.
473 Gunderson CC, Fader AN, Carson KA & Bristow RE 2012 Oncologic and reproductive
474 outcomes with progestin therapy in women with endometrial hyperplasia and grade 1
475 adenocarcinoma: a systematic review. *Gynecol Oncol* **125** 477-482.
476 Jakubowicz DJ, Seppala M, Jakubowicz S, Rodriguez-Armas O, Rivas-Santiago A, Koistinen
477 H, Koistinen R & Nestler JE 2001 Insulin reduction with metformin increases luteal phase
478 serum glycodelin and insulin-like growth factor-binding protein 1 concentrations and
479 enhances uterine vascularity and blood flow in the polycystic ovary syndrome. *J Clin*
480 *Endocrinol Metab* **86** 1126-1133.
481 Kim HJ, Lee GS, Ji YK, Choi KC & Jeung EB 2006 Differential expression of uterine
482 calcium transporter 1 and plasma membrane Ca2+ ATPase 1b during rat estrous cycle. *Am J*
483 *Physiol Endocrinol Metab* **291** E234-241.
484 Kim JY, Song H, Kim H, Kang HJ, Jun JH, Hong SR, Koong MK & Kim IS 2009
485 Transcriptional profiling with a pathway-oriented analysis identifies dysregulated molecular
486 phenotypes in the endometrium of patients with polycystic ovary syndrome. *J Clin*
487 *Endocrinol Metab* **94** 1416-1426.

488 Knox KL, Ringstrom SJ, Szabo M, Perlyn CA, Sutandi S & Schwartz NB 1996 RU486 on an
489 estrogen background blocks the rise in serum follicle-stimulating hormone induced by
490 antiserum to inhibin or ovariectomy. *Endocrinology* **137** 1226-1232.
491 Lan CW, Chen MJ, Tai KY, Yu DC, Yang YC, Jan PS, Yang YS, Chen HF & Ho HN 2015
492 Functional microarray analysis of differentially expressed genes in granulosa cells from
493 women with polycystic ovary syndrome related to MAPK/ERK signaling. *Sci Rep* **5** 14994.
494 Lee CH, Kim TH, Lee JH, Oh SJ, Yoo JY, Kwon HS, Kim YI, Ferguson SD, Ahn JY, Ku BJ
495 *et al.* 2013 Extracellular signal-regulated kinase 1/2 signaling pathway is required for
496 endometrial decidualization in mice and human. *PLoS One* **8** e75282.
497 Li X, Cui P, Jiang HY, Guo YR, Pishdari B, Hu M, Feng Y, Billig H & Shao R 2015
498 Reversing the reduced level of endometrial GLUT4 expression in polycystic ovary syndrome:
499 a mechanistic study of metformin action. *Am J Transl Res* **7** 574-586.
500 Li X, Feng Y, Lin JF, Billig H & Shao R 2014a Endometrial progesterone resistance and
501 PCOS. *J Biomed Sci* **21** 2.
502 Li X, Guo JR, Lin JF, Feng Y, Billig H & Shao R 2014b Combination of Diane-35 and
503 metformin to treat early endometrial carcinoma in PCOS women with insulin resistance *J*
504 *Cancer* **5** 173-181.
505 Liu M, Gao J, Zhang Y, Li P, Wang H, Ren X & Li C 2015 Serum levels of TSP-1, NF-
506 kappaB and TGF-beta1 in polycystic ovarian syndrome (PCOS) patients in northern China
507 suggest PCOS is associated with chronic inflammation. *Clin Endocrinol (Oxf)* **83** 913-922.
508 Lopes IM, Maganhin CC, Oliveira-Filho RM, Simoes RS, Simoes MJ, Iwata MC, Baracat EC
509 & Soares JM, Jr. 2014 Histomorphometric Analysis and Markers of Endometrial Receptivity
510 Embryonic Implantation in Women With Polycystic Ovary Syndrome During the Treatment
511 With Progesterone. *Reprod Sci* **21** 930-938.
512 Margarit L, Taylor A, Roberts MH, Hopkins L, Davies C, Brenton AG, Conlan RS,
513 Bunkheila A, Joels L, White JO *et al.* 2010 MUC1 as a discriminator between endometrium
514 from fertile and infertile patients with PCOS and endometriosis. *J Clin Endocrinol Metab* **95**
515 5320-5329.
516 Matteo M, Serviddio G, Massenzio F, Scillitani G, Castellana L, Picca G, Sanguedolce F,
517 Cignarelli M, Altomare E, Bufo P *et al.* 2010 Reduced percentage of natural killer cells
518 associated with impaired cytokine network in the secretory endometrium of infertile women
519 with polycystic ovary syndrome. *Fertil Steril* **94** 2222-2227, 2227 e2221-2223.
520 Mukherjee A, Amato P, Allred DC, DeMayo FJ & Lydon JP 2007 Steroid receptor
521 coactivator 2 is required for female fertility and mammary morphogenesis: insights from the
522 mouse, relevance to the human. *Nucl Recept Signal* **5** e011.
523 Mukherjee A, Soyal SM, Fernandez-Valdivia R, Gehin M, Chambon P, Demayo FJ, Lydon
524 JP & O'Malley BW 2006 Steroid receptor coactivator 2 is critical for progesterone-dependent
525 uterine function and mammary morphogenesis in the mouse. *Mol Cell Biol* **26** 6571-6583.
526 Naderpoor N, Shorakae S, de Courten B, Misso ML, Moran LJ & Teede HJ 2015 Metformin
527 and lifestyle modification in polycystic ovary syndrome: systematic review and meta-analysis.
528 *Hum Reprod Update* **21** 560-574.
529 Nelson-Degrave VL, Wickenheisser JK, Hendricks KL, Asano T, Fujishiro M, Legro RS,
530 Kimball SR, Strauss JF, 3rd & McAllister JM 2005 Alterations in mitogen-activated protein
531 kinase kinase and extracellular regulated kinase signaling in theca cells contribute to
532 excessive androgen production in polycystic ovary syndrome. *Mol Endocrinol* **19** 379-390.
533 Orostica L, Astorga I, Plaza-Parrochia F, Vera C, Garcia V, Carvajal R, Gabler F, Romero C
534 & Vega M 2016 Proinflammatory environment and role of TNF-alpha in endometrial function
535 of obese women having polycystic ovarian syndrome. *Int J Obes (Lond)* **40** 1715-1722.
536 Palomba S, de Wilde MA, Falbo A, Koster MP, La Sala GB & Fauser BC 2015 Pregnancy
537 complications in women with polycystic ovary syndrome. *Hum Reprod Update* **21** 575-592.

538 Palomba S, Russo T, Orio F, Jr., Falbo A, Manguso F, Cascella T, Tolino A, Carmina E,
539 Colao A & Zullo F 2006 Uterine effects of metformin administration in anovulatory women
540 with polycystic ovary syndrome. *Hum Reprod* **21** 457-465.
541 Patel B, Elguero S, Thakore S, Dahoud W, Bedaiwy M & Mesiano S 2015 Role of nuclear
542 progesterone receptor isoforms in uterine pathophysiology. *Hum Reprod Update* **21** 155-173.
543 Piltonen TT 2016 Polycystic ovary syndrome: Endometrial markers. *Best Pract Res Clin*
544 *Obstet Gynaecol* **37** 66-79.
545 Piltonen TT, Chen J, Erikson DW, Spitzer TL, Barragan F, Rabban JT, Huddleston H, Irwin
546 JC & Giudice LC 2013 Mesenchymal stem/progenitors and other endometrial cell types from
547 women with polycystic ovary syndrome (PCOS) display inflammatory and oncogenic
548 potential. *J Clin Endocrinol Metab* **98** 3765-3775.
549 Piltonen TT, Chen JC, Khatun M, Kangasniemi M, Liakka A, Spitzer T, Tran N, Huddleston
550 H, Irwin JC & Giudice LC 2015 Endometrial stromal fibroblasts from women with polycystic
551 ovary syndrome have impaired progesterone-mediated decidualization, aberrant cytokine
552 profiles and promote enhanced immune cell migration in vitro. *Hum Reprod* **30** 1203-1215.
553 Poretsky L, Clemons J & Bogovich K 1992 Hyperinsulinemia and human chorionic
554 gonadotropin synergistically promote the growth of ovarian follicular cysts in rats.
555 *Metabolism* **41** 903-910.
556 Quezada S, Avellaira C, Johnson MC, Gabler F, Fuentes A & Vega M 2006 Evaluation of
557 steroid receptors, coregulators, and molecules associated with uterine receptivity in secretory
558 endometria from untreated women with polycystic ovary syndrome. *Fertil Steril* **85** 1017-
559 1026.
560 Rosenfield RL & Ehrmann DA 2016 The Pathogenesis of Polycystic Ovary Syndrome
561 (PCOS): The Hypothesis of PCOS as Functional Ovarian Hyperandrogenism Revisited.
562 *Endocr Rev* **37** 467-520.
563 Savaris RF, Groll JM, Young SL, DeMayo FJ, Jeong JW, Hamilton AE, Giudice LC &
564 Lessey BA 2011 Progesterone resistance in PCOS endometrium: a microarray analysis in
565 clomiphene citrate-treated and artificial menstrual cycles. *J Clin Endocrinol Metab* **96** 1737-
566 1746.
567 Shao R, Cao S, Wang X, Feng Y & Billig H 2014a The elusive and controversial roles of
568 estrogen and progesterone receptors in human endometriosis. *Am J Transl Res* **6** 104-113.
569 Shao R, Li X, Feng Y, Lin JF & Billig H 2014b Direct effects of metformin in the
570 endometrium: a hypothetical mechanism for the treatment of women with PCOS and
571 endometrial carcinoma. *J Exp Clin Cancer Res* **33** 41.
572 Tapia-Pizarro A, Archiles S, Argandona F, Valencia C, Zavaleta K, Cecilia Johnson M,
573 Gonzalez-Ramos R & Devoto L 2017 hCG activates Epac-Erk1/2 signaling regulating
574 Progesterone Receptor expression and function in human endometrial stromal cells. *Mol Hum*
575 *Reprod* **23** 393-405.
576 Thienel T, Chwalisz K & Winterhager E 2002 Expression of MAPkinases (Erk1/2) during
577 decidualization in the rat: regulation by progesterone and nitric oxide. *Mol Hum Reprod* **8**
578 465-474.
579 Tranguch S, Wang H, Daikoku T, Xie H, Smith DF & Dey SK 2007 FKBP52 deficiency-
580 conferred uterine progesterone resistance is genetic background and pregnancy stage specific.
581 *J Clin Invest* **117** 1824-1834.
582 Vrbikova J & Cibula D 2005 Combined oral contraceptives in the treatment of polycystic
583 ovary syndrome. *Hum Reprod Update* **11** 277-291.
584 Wira CR, Fahey JV, Sentman CL, Pioli PA & Shen L 2005 Innate and adaptive immunity in
585 female genital tract: cellular responses and interactions. *Immunol Rev* **206** 306-335.

586 Yang Z, Wolf IM, Chen H, Periyasamy S, Chen Z, Yong W, Shi S, Zhao W, Xu J, Srivastava
587 A *et al.* 2006 FK506-binding protein 52 is essential to uterine reproductive physiology
588 controlled by the progesterone receptor A isoform. *Mol Endocrinol* **20** 2682-2694.
589 Zhang Y, Hu M, Meng F, Sun X, Xu H, Zhang J, Cui P, Morina N, Li X, Li W *et al.* 2017
590 Metformin Ameliorates Uterine Defects in a Rat Model of Polycystic Ovary Syndrome.
591 *EBioMedicine* **18** 157-170.
592 Zhang Y, Meng F, Sun X, Sun X, Hu M, Cui P, Vestin E, Li X, Li W, Wu XK *et al.* 2018
593 Hyperandrogenism and insulin resistance contribute to hepatic steatosis and inflammation in
594 female rat liver. *Oncotarget* **In Press**.
595 Zhang Y, Sun X, Sun X, Meng F, Hu M, Li X, Li W, Wu XK, Brännström M, Shao R *et al.*
596 2016 Molecular characterization of insulin resistance and glycolytic metabolism in the rat
597 uterus. *Sci Rep* **6** 30679.
598 Zhao Y, Zhang C, Huang Y, Yu Y, Li R, Li M, Liu N, Liu P & Qiao J 2015 Up-regulated
599 expression of WNT5a increases inflammation and oxidative stress via PI3K/AKT/NF-kappaB
600 signaling in the granulosa cells of PCOS patients. *J Clin Endocrinol Metab* **100** 201-211.

601

602

1 **Figure legends**

2 **Figure 1. Chronic treatment with metformin alters PGR isoform protein expression and**
3 **PGR-target gene expression in the rat uterus *in vivo*.** A, Western blot analysis of protein
4 expression in the rat uterus was performed. Representative images and quantification of the
5 densitometric data (n = 8–9/group) of PGR isoforms are shown. B, Immunohistochemical
6 detection of PGRA/B in control rats treated with saline or metformin and in insulin+hCG-
7 treated rats treated with saline or metformin. Representative images (n = 5/group) are shown.
8 Lu, lumen; Le, luminal epithelial cells; Ge, glandular epithelial cells; Str, stromal cells. Scale
9 bars (100 μm) are indicated in the photomicrographs. High magnification images are shown
10 in the bottom panels. C, Uterine tissues from control rats treated with vehicle or metformin
11 and insulin+hCG-treated rats treated with saline or metformin (n = 6/group) were analyzed for
12 mRNA levels of *Ihh*, *Ptch*, *Smo*, *Nr2f2*, *Hand2*, *Fkbp52*, and *Ncoa2* by qRT-PCR. The
13 mRNA level of each gene relative to the mean of the sum of the *Gapdh* and *U87* mRNA
14 levels in the same sample is shown. Values are expressed as means ± SEM. Statistical tests
15 are described in the Material and Methods. * $p < 0.05$; ** $p < 0.01$; *** $p < 0.001$.

16 **Figure 2. Chronic treatment with metformin alters PGR isoform protein expression and**
17 **PGR-target gene expression in the rat uterus after implantation.** A, Western blot analysis
18 of protein expression in the rat uterus was performed. Representative images and
19 quantification of the densitometric data of PR isoforms are shown (n = 5–7/group). B,
20 Immunohistochemical detection of PGRA/B in the uterine implantation and inter-implantation
21 sites. Representative images are shown (n = 5/group). DS, decidualized stroma; Lu, lumen;
22 Le, luminal epithelial cells; Ge, glandular epithelial cells; Str, stromal cells. Scale bars (100
23 μm) are indicated in the photomicrographs. C, Uterine tissues (n = 5–6/group) were analyzed
24 for mRNA levels of *Ihh*, *Ptch*, *Smo*, *Nr2f2*, *Hand2*, *Fkbp52*, and *Ncoa2* by qRT-PCR. The
25 mRNA level of each gene is shown relative to the mean of the sum of the *Gapdh* and *U87*

26 mRNA levels in the same sample. Values are expressed as means ± SEM. Statistical tests are
27 described in the Materials and Methods. * $p < 0.05$; ** $p < 0.01$; *** $p < 0.001$.

28 **Figure 3. Specific regulation of uterine PGR isoforms, PGR-targeted and implantation-**
29 **related gene expression by metformin treatment *in vitro*.** Quantitative RT-PCR analysis of
30 (A) *Pgr*, *Pgrb*, *Ihh*, *Ptch*, *Smo*, *Nr2f2*, *Hand2*, *Fkbp52*, and *Ncoa2* and (B) *Prl*, *Igfbp1*, *Lif*,
31 *Il11*, *Pc6*, *Spp1*, *Maoa*, *Ednrb*, *Hoxa10*, *Hoxa11*, *Lrh1*, *Sgk1*, *Hbegf*, and *Krt13* mRNA levels
32 in rat uterine tissues treated with either saline or 10 mM metformin for the indicated culture
33 times (n = 6/group). mRNA levels were normalized to the average levels of *Gapdh* and *U87*
34 mRNA in the same sample. Values are expressed as means ± SEM. Statistical tests are
35 described in the Materials and Methods. * $p < 0.05$; ** $p < 0.01$; *** $p < 0.001$.

36 **Figure 4. Specific regulation of uterine PGR isoforms and PGR-targeted gene expression**
37 **by treatment with P4 and/or RU486 *in vivo*.** Uterine tissues (n = 5–6/group) were analyzed
38 for mRNA levels of *Pgr*, *Pgrb*, *Ihh*, *Ptch*, *Smo*, *Nr2f2*, *Hand2*, *Fkbp52*, and *Ncoa2* by qRT-
39 PCR. mRNA levels were normalized to the average levels of *Gapdh* and *U87* mRNA in the
40 same sample. Values are expressed as means ± SEM. Statistical tests are described in the
41 Materials and Methods. * $p < 0.05$; ** $p < 0.01$; *** $p < 0.001$.

42 **Figure 5. Chronic treatment with metformin alters the MAPK signaling pathway in the**
43 **rat uterus before and after implantation.** Western blot analysis of protein expression in the
44 rat uterus was performed. Representative images and quantification of the densitometric data
45 for p-c-Raf, p-MEK1/2, p-ERK1/2, ERK1/2, p-p38 MAPK, and p38 MAPK are shown (n =
46 6–9/group before implantation; n = 5–6/group after implantation). Values are expressed as
47 means ± SEM. Statistical tests are described in the Materials and Methods. * $p < 0.05$; ** $p <$
48 $0.01$.

49 **Figure 6. Chronic treatment with metformin alters ER subtype mRNA and protein**
50 **expression in the rat uterus *in vivo*.** A, Uterine tissues from control rats treated with saline

51 vehicle or metformin and insulin+hCG-treated rats treated with saline or metformin (n =
52 6/group) were analyzed for mRNA levels of *Esr1* (ERα) and *Esr2* (ERβ) by qRT-PCR. The
53 mRNA level of each gene relative to the mean of the sum of the *Gapdh* and *U87* mRNA
54 levels in the same sample is shown. Values are expressed as means ± SEM. Statistical tests
55 are described in the Material and Methods. * $p < 0.05$; ** $p < 0.01$; *** $p < 0.001$. B,
56 Immunofluorescence detection of ERα (red) and ERβ (green) in control rats treated with
57 saline (B1-2) or metformin (C1-2) and in insulin+hCG-treated rats treated with saline (D1-2)
58 or metformin (E1-2). Representative images are shown (n = 5/group). Cell nuclei were
59 counterstained with DAPI (blue, lower panel). Lu, lumen; Le, luminal epithelial cells; Ge,
60 glandular epithelial cells; Str, stromal cells. Scale bars (100 μm) are indicated in the
61 photomicrographs.

62 **Figure 7. Chronic treatment with metformin alters ER subtype mRNA and protein**
63 **expression in the rat uterus after implantation.** A, Uterine tissues from control rats treated
64 with saline or metformin and insulin+hCG-treated rats treated with saline or metformin (n =
65 5/group) were analyzed for mRNA levels of *Esr1* (ERα) and *Esr2* (ERβ) by qRT-PCR. The
66 mRNA level of each gene relative to the mean of the sum of the *Gapdh* and *U87* mRNA
67 levels in the same sample is shown. Values are expressed as means ± SEM. Statistical tests
68 are described in the Materials and Methods. * $p < 0.05$; ** $p < 0.01$. B, Immunofluorescence
69 detection of ERα (red) and ERβ (green) in control rats treated with saline (B1-2) or metformin
70 (C1-2) and in insulin+hCG-treated rats treated with metformin with implantation (D1-2) or
71 without implantation (E1). Representative images are shown (n = 5/group). Cell nuclei were
72 counterstained with DAPI (blue, lower panel). DS, decidualized stroma; Lu, lumen; Le,
73 luminal epithelial cells; Ge, glandular epithelial cells; Str, stromal cells. Scale bars (100 μm)
74 are indicated in the photomicrographs.

75 **Figure 8.** Schematic representation of the actions of metformin on the uterine progesterone
76 signaling in the PCOS-like rats. Note that bold symbol indicates metformin-regulated genes
77 and proteins and asterisk indicates that treatment with metformin or progesterone share the
78 same targeted genes and proteins.
79
80 **Supplementary Figure 1. Schematic representation of experimental groups and**
81 **treatment protocol.** n, the final number of animals.
82 **Supplementary Figure 2. Photographs and illustration of the procedures for rat uterine**
83 **tissue preparation and culture with and without metformin.** Culture media with and
84 without metformin treatment were changed daily.
85 **Supplementary Figure 3. Effects of metformin on uterine structure in rats after**
86 **implantation.** Female rats were mated individually with fertile male rats according to their
87 estrous cycle stage. Representative photomicrographs of uteri collected on day 6 after
88 pregnancy with implantation sites visualized by Chicago Blue B dye injection. Because the
89 insulin+hCG-treated rats without a normal estrous cycle display implantation failure, these
90 rats treated with saline were excluded from the analysis. Higher-magnification images of the
91 different areas are shown on the rightmost three panels of each row. MD, mesometrial
92 decidua; AD, antimesometrial decidua; En, endometrium; Myo, myometrium. Scale bars (100
93 μm) are indicated in the photomicrographs.
94 **Supplementary Figure 4. Chronic treatment with metformin alters p-histone H3 (Ser10)**
95 **protein expression in the rat uterus *in vivo*.** Immunofluorescence detection of p-histone H3
96 (red) in control rats treated with saline (A1-4) or metformin (B1-4) and in insulin+hCG-
97 treated rats treated with saline (C1-4) or metformin (D1-4). Cell nuclei were counterstained
98 with DAPI (blue). Lu, lumen; Le, luminal epithelial cells; Ge, glandular epithelial cells; Str,
99 stromal cells; M, myometrium. Scale bars (100 μm) are indicated in the photomicrographs.

100 The number of all p-histone H3-positive cells in whole luminal epithelial cells, glandular
101 epithelial/stromal cells and myometrium)/uterine section/animal was counted. Semi-
102 quantitative immunofluorescence of p-histone H3 (Q-H score) in the different uterine cell
103 types (n = 5/group) is shown in E. Values are expressed as means ± SEM. Statistical tests are
104 described in the Material and Methods. * $p < 0.05$.

105 **Supplementary Figure 5. Chronic treatment with metformin alters p-histone H3 (Ser10)**
106 **protein expression in the rat uterus after implantation.** Immunofluorescence detection of
107 p-histone H3 (red) in control rats treated with saline (A1-4) or metformin (B1-4) and in
108 insulin+hCG-treated rats treated with metformin with implantation (C1-4) or without
109 implantation (D1-2). Cell nuclei were counterstained with DAPI (blue). DS, decidualized
110 stroma; Le, luminal epithelial cells; Ge, glandular epithelial cells; Str, stromal cells; M,
111 myometrium. Scale bars (100 μm) are indicated in the photomicrographs. The number of all
112 p-histone H3-positive cells in whole luminal epithelial cells, glandular epithelial/stromal cells
113 and myometrium)/uterine section/animal was counted. Semi-quantitative immunofluorescence
114 of p-histone H3 (Q-H score) in the different uterine cell types is shown in E. Uterine tissues
115 were analyzed (n = 8/group; n = 5 for insulin+hCG-treated rats with metformin but without
116 implantation). Values are expressed as means ± SEM. Statistical tests are described in the
117 Materials and Methods. * $p < 0.05$; ** $p < 0.01$.

118

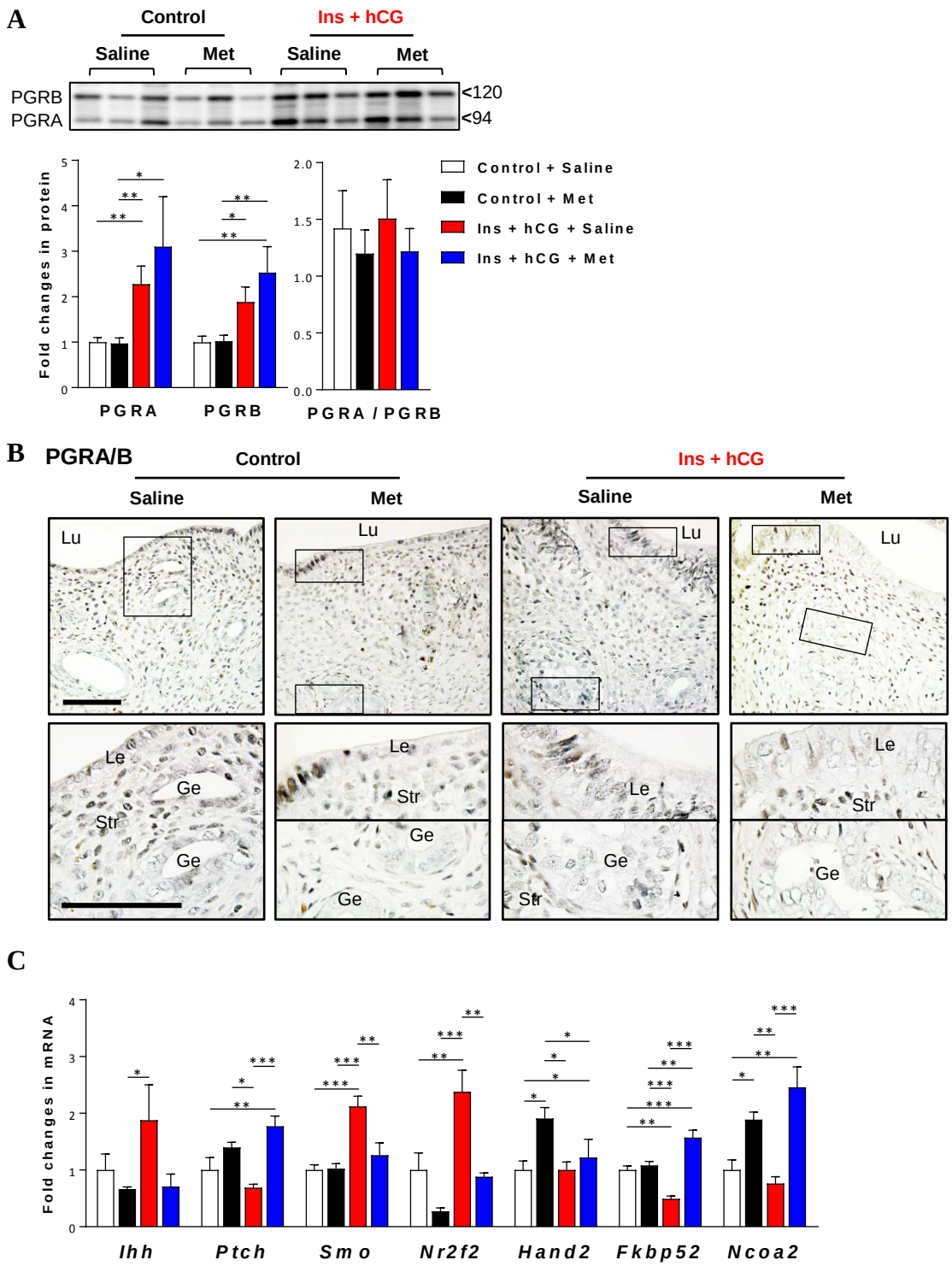
A
Control
Ins + hCG
Saline
Met
Saline
Met
PGRB
PGRA
<120
<94
Fold changes in protein
PGRA
PGRB
PGRA / PGRB
Control + Saline
Control + Met
Ins + hCG + Saline
Ins + hCG + Met
B
PGRA/B
Control
Ins + hCG
Saline
Met
Saline
Met
Lu
Le
Ge
Str
C
Fold changes in mRNA
Ihh
Ptch
Smo
Nr2f2
Hand2
Fkbp52
Ncoa2

Figure 2

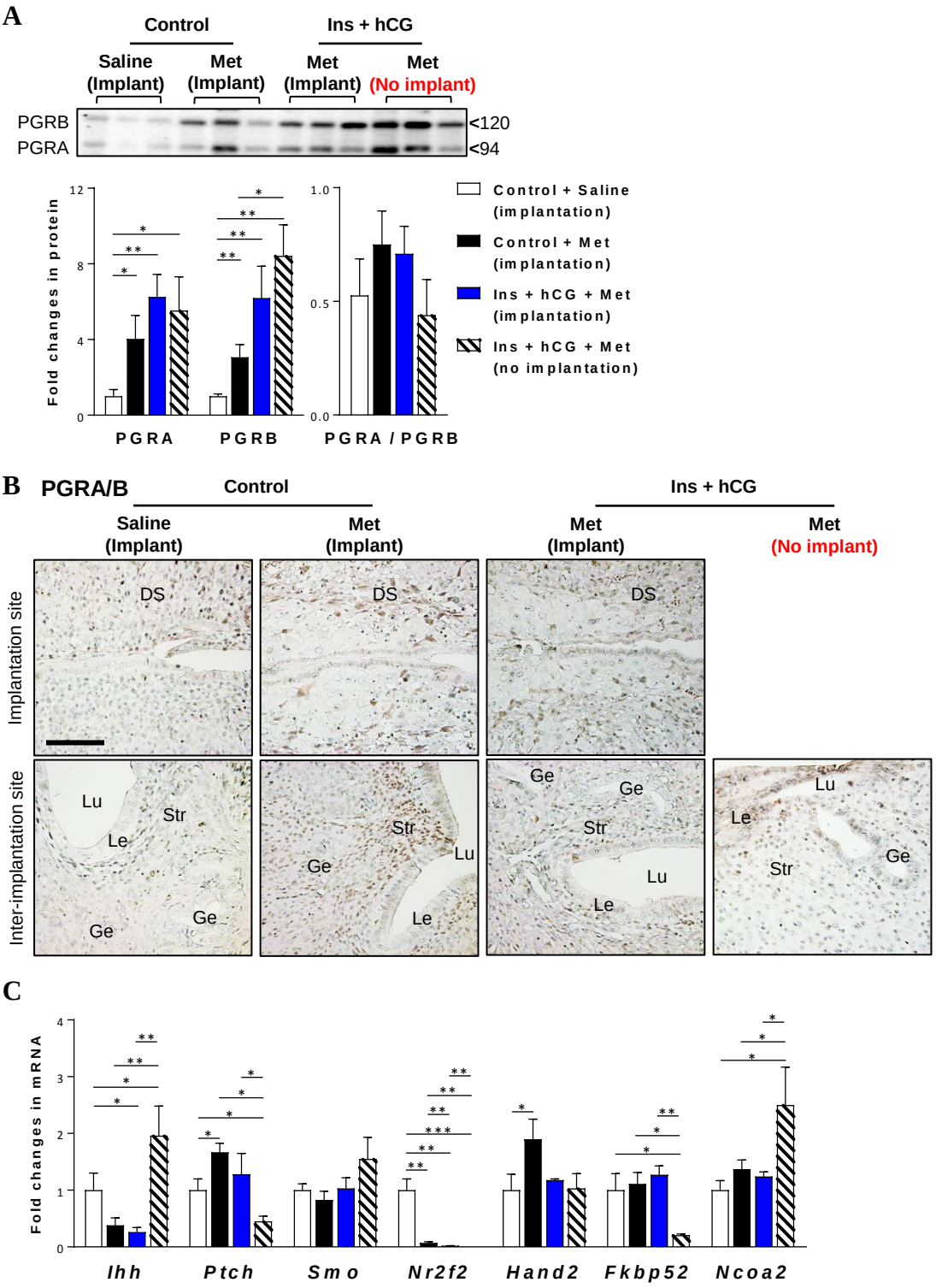
A
Control
Ins + hCG
Saline (Implant)
Met (Implant)
Met (Implant)
Met (No implant)
PGRB
PGRA
<120
<94
Fold changes in protein
PGRA
PGRB
PGRA / PGRB
Control + Saline (implantation)
Control + Met (implantation)
Ins + hCG + Met (implantation)
Ins + hCG + Met (no implantation)
B
PGRA/B
Control
Ins + hCG
Saline (Implant)
Met (Implant)
Met (Implant)
Met (No implant)
Implantation site
Inter-implantation site
DS
Lu
Le
Str
Ge
C
Fold changes in mRNA
Ihh
Ptch
Smo
Nr2f2
Hand2
Fkbp52
Ncoa2

Figure 3



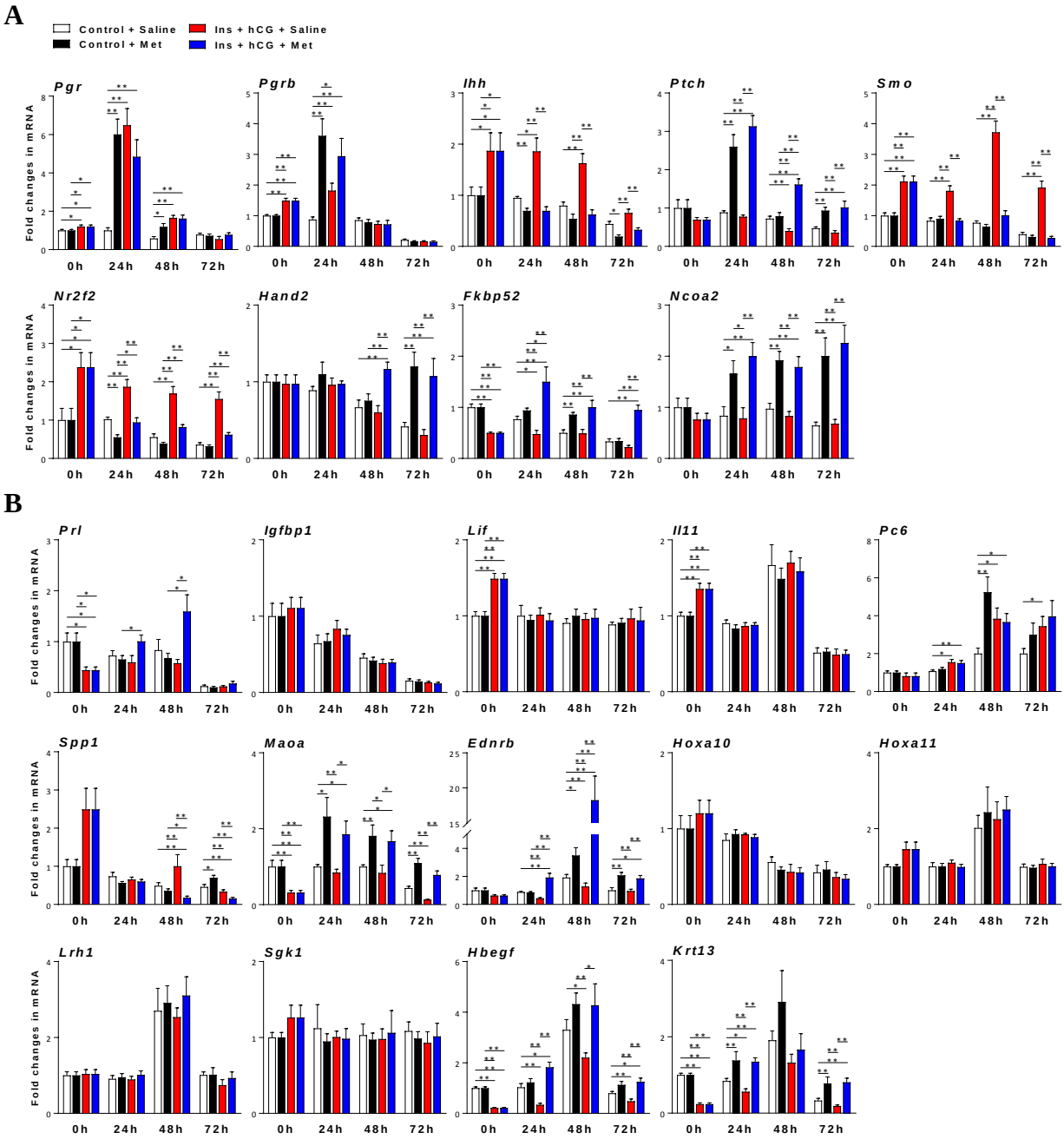
A
Control + Saline
Control + Met
Ins + hCG + Saline
Ins + hCG + Met
Pgr
Pgrb
Ihh
Ptch
Smo
Nr2f2
Hand2
Fkbp52
Ncoa2
Fold changes in mRNA
0h
24h
48h
72h
B
Prl
Igfbp1
Lif
Il11
Pc6
Spp1
Maoa
Ednrb
Hoxa10
Hoxa11
Lrh1
Sgk1
Hbegf
Krt13

Figure 4



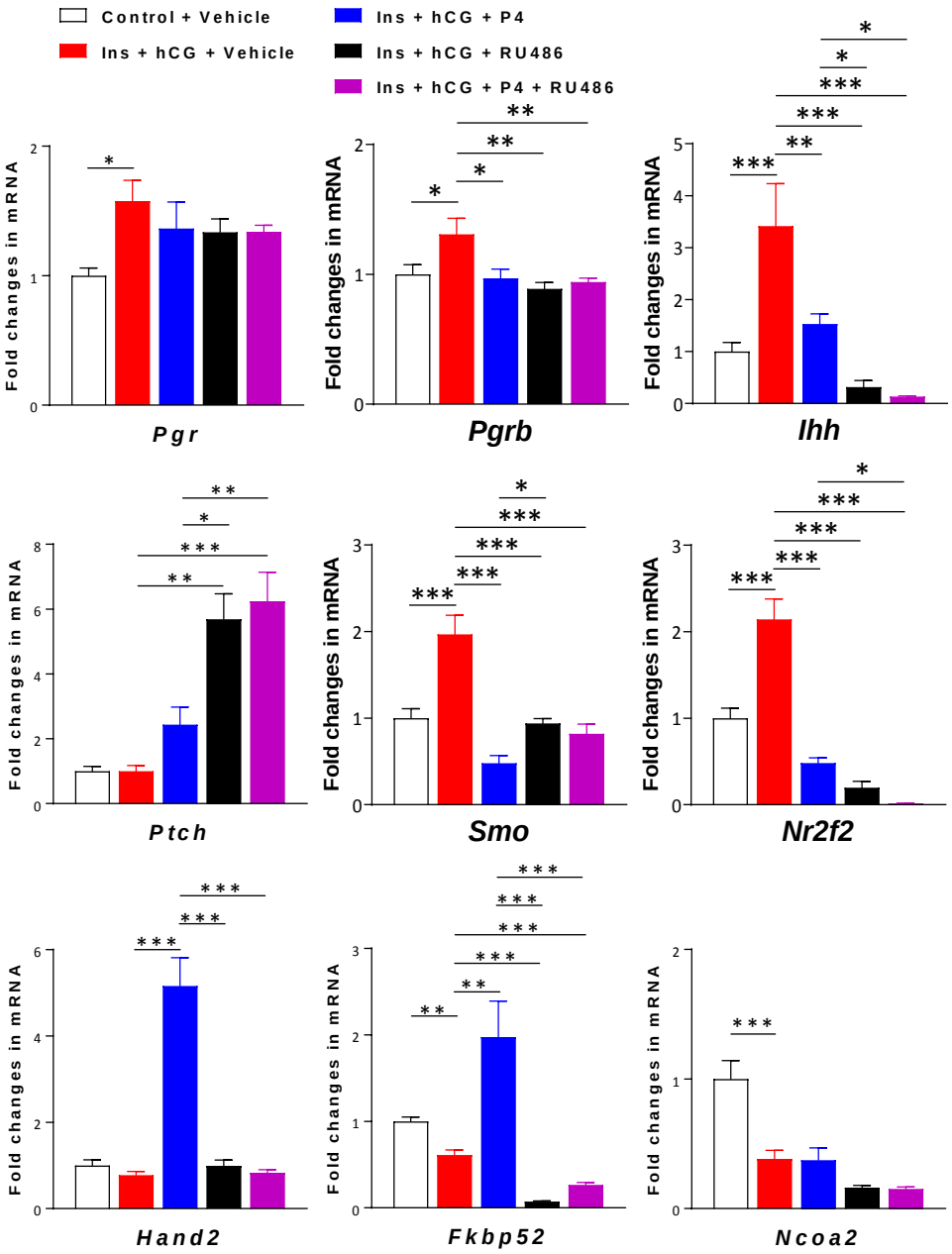
Control + Vehicle
Ins + hCG + Vehicle
Ins + hCG + P4
Ins + hCG + RU486
Ins + hCG + P4 + RU486
Fold changes in mRNA
Pgr
Pgrb
Ihh
Ptch
Smo
Nr2f2
Hand2
Fkbp52
Ncoa2

Figure 5



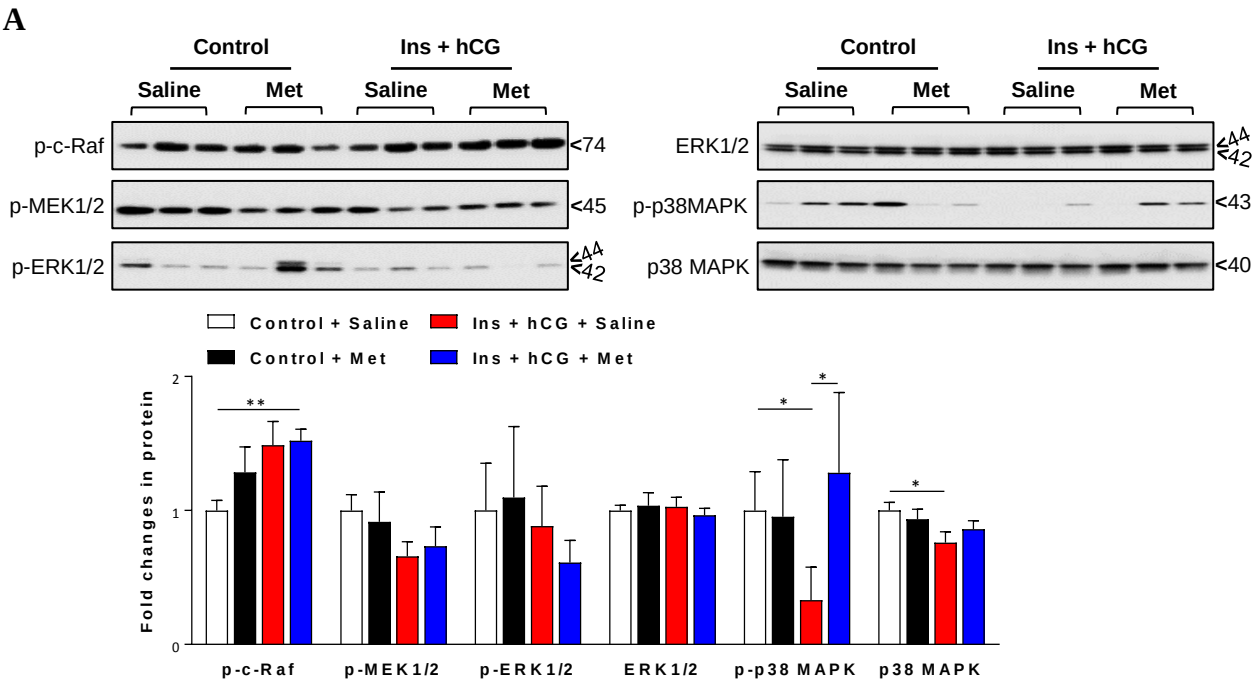
A
Control
Ins + hCG
Saline
Met
Saline
Met
p-c-Raf
p-MEK1/2
p-ERK1/2
<74
<45
<44
<42
ERK1/2
p-p38MAPK
p38 MAPK
<43
<40
Control + Saline
Ins + hCG + Saline
Control + Met
Ins + hCG + Met
Fold changes in protein
p-c-Raf
p-MEK1/2
p-ERK1/2
ERK1/2
p-p38 MAPK
p38 MAPK

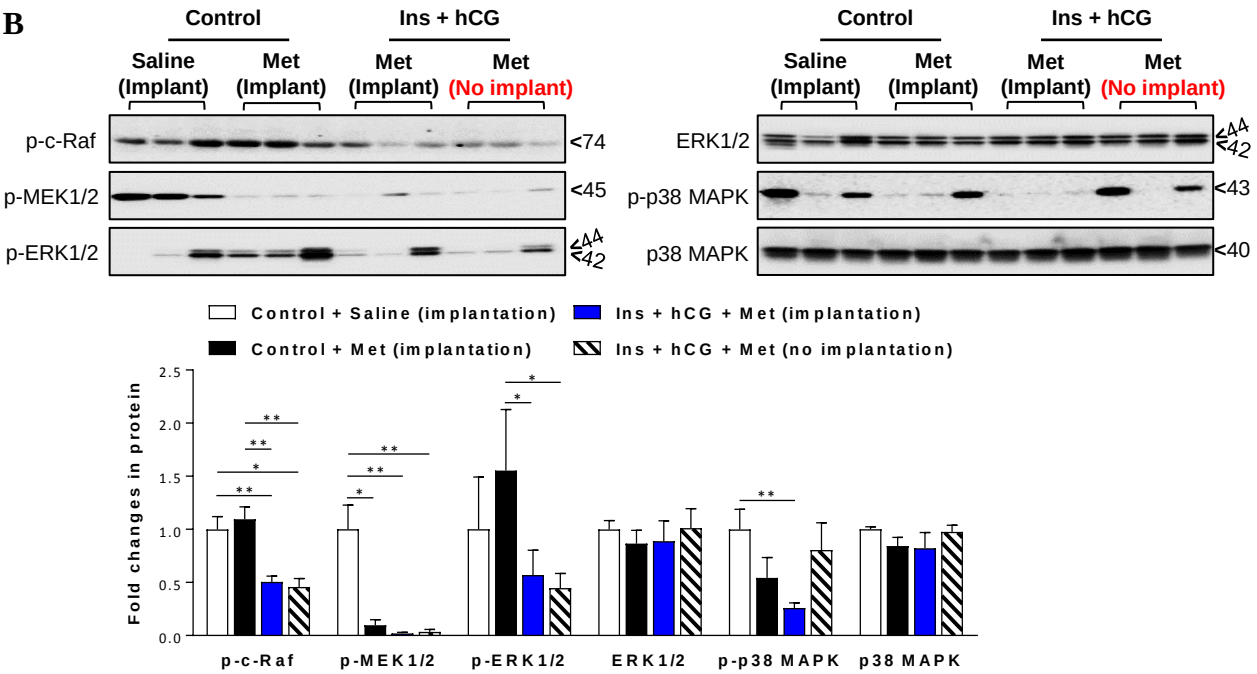
B
Control
Ins + hCG
Saline (Implant)
Met (Implant)
Met (Implant)
Met (No implant)
p-c-Raf
p-MEK1/2
p-ERK1/2
<74
<45
<44
<42
ERK1/2
p-p38 MAPK
p38 MAPK
<43
<40
Control + Saline (implantation)
Ins + hCG + Met (implantation)
Control + Met (implantation)
Ins + hCG + Met (no implantation)
Fold changes in protein
p-c-Raf
p-MEK1/2
p-ERK1/2
ERK1/2
p-p38 MAPK
p38 MAPK

Figure 6



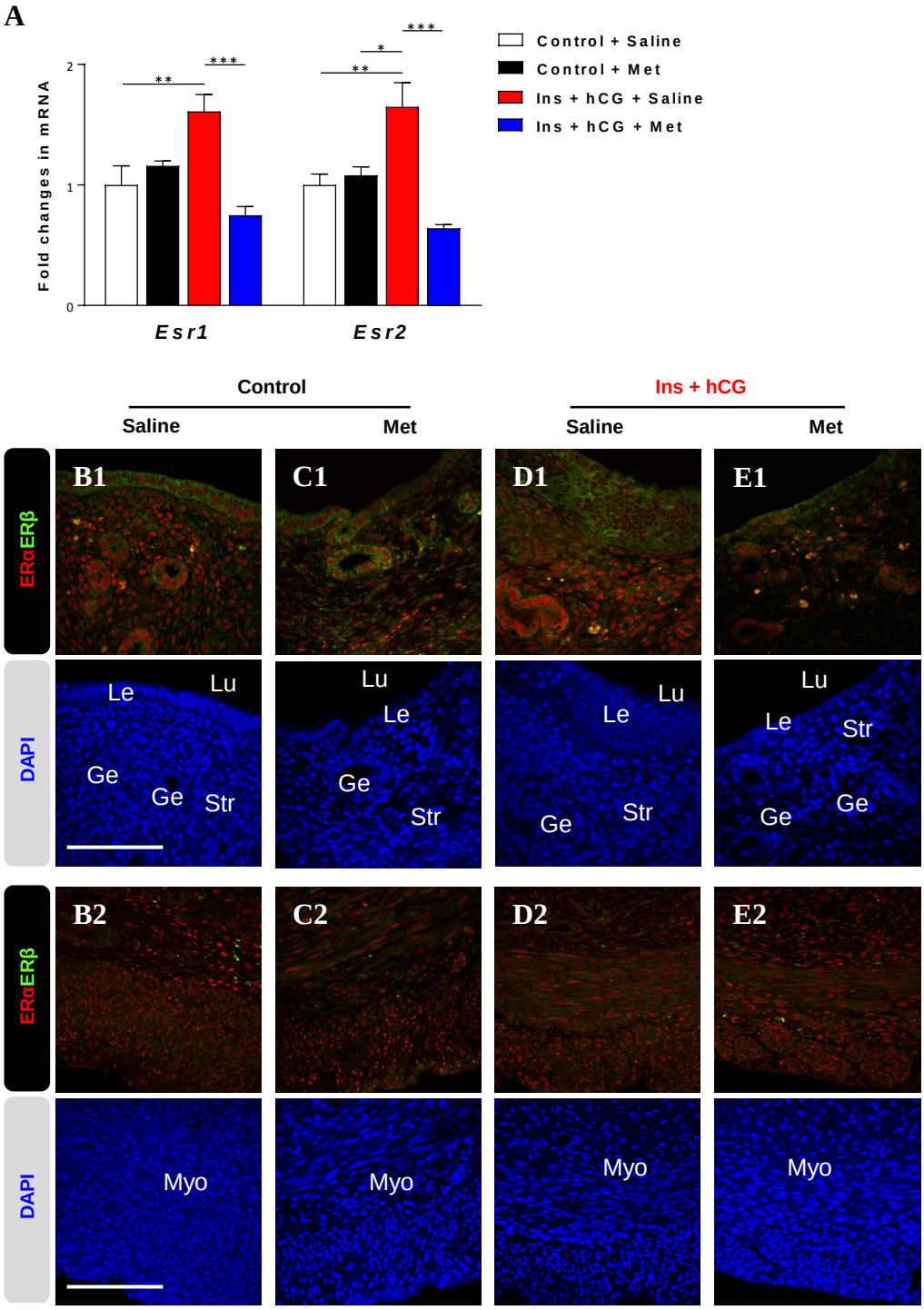
A
Fold changes in mRNA
0
1
2
**
***
**
*
***
Esr1
Esr2
Control + Saline
Control + Met
Ins + hCG + Saline
Ins + hCG + Met
Control
Ins + hCG
Saline
Met
Saline
Met
ERαERβ
DAPI
B1
C1
D1
E1
Le
Lu
Ge
Str
B2
C2
D2
E2
Myo

Figure 7



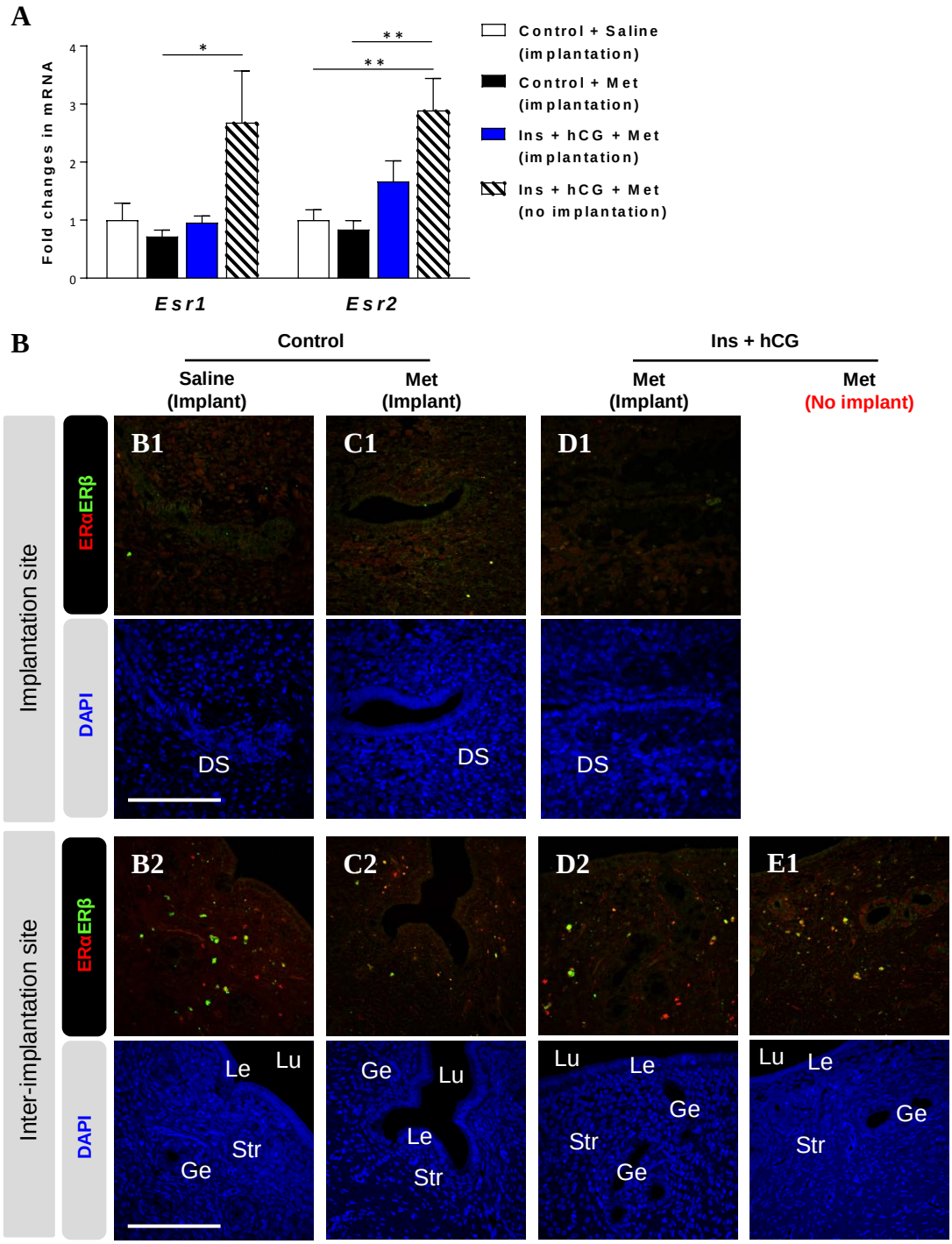
A
Fold changes in mRNA
0
1
2
3
4
*
**
**
Esr1
Esr2
Control + Saline (implantation)
Control + Met (implantation)
Ins + hCG + Met (implantation)
Ins + hCG + Met (no implantation)
B
Control
Ins + hCG
Saline (Implant)
Met (Implant)
Met (Implant)
Met (No implant)
Implantation site
Inter-implantation site
ERαERβ
DAPI
B1
C1
D1
B2
C2
D2
E1
DS
Le
Lu
Ge
Str

Figure 8



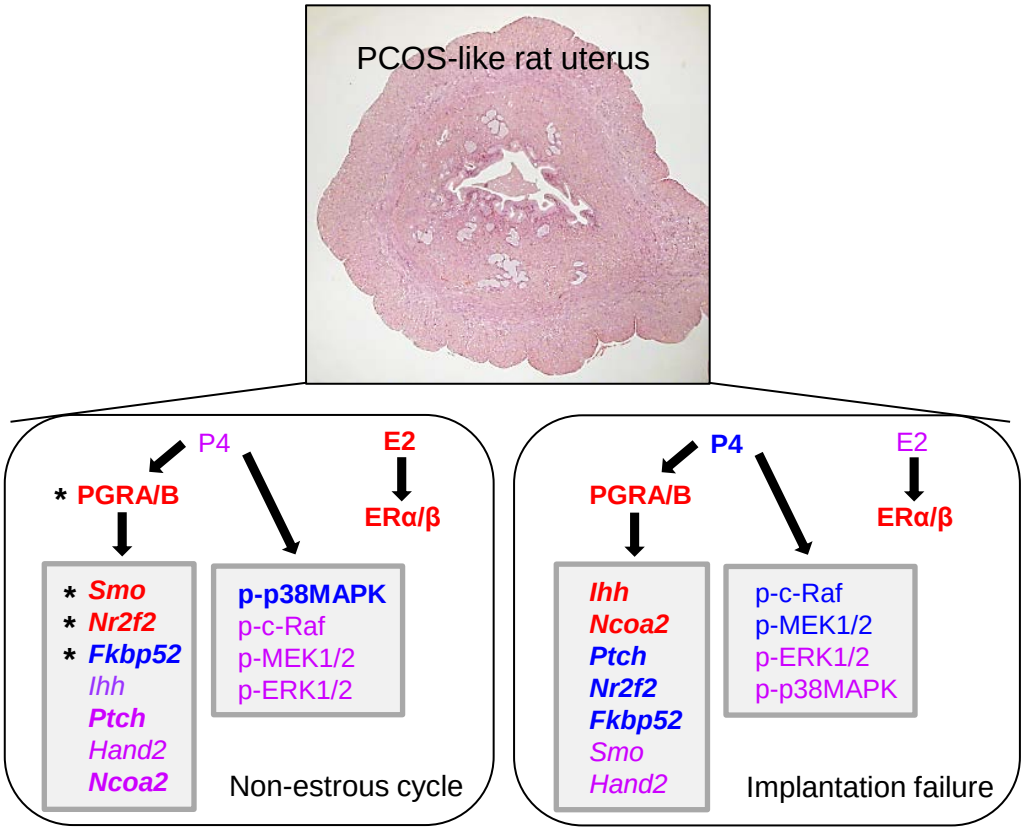


Increased expression Decreased expression Unchanged expression

Suppl MM

## Materials and Methods

### *Primary in vitro tissue culture and treatment*

Uterine tissue culture and treatment was essentially carried out as described previously (Cui *et al.* 2015; Li *et al.* 2015). After rinsing in cold PBS, uterine tissues obtained from control (n = 5) and PCOS-like (n = 5) rats were divided into equal-sized explants and placed in 24-well tissue culture plates (Sarstedt, Newton, MA) containing RPMI-1640 medium with charcoal-stripped 10% fetal calf serum and 100 IU/ml penicillin/streptomycin (GIBCO-BRL, San Francisco, CA). Cultured tissues treated with sterile saline or metformin (10 mM in sterile saline) were incubated in a humidified incubator (37ºC, 95% $O_2$, 5% $CO_2$) and separately collected at 0 h, 24 h, 48 h, and 72 h after treatment (Supplemental Fig. 2). Each culture condition was performed in five replicates (five wells), and tissues from a minimum of five control rats and five PCOS-like (insulin+hCG-treated) rats were used. At the end of the experiments, cultured tissues were snap-frozen in liquid nitrogen and stored at –70°C.

### *Morphological assessment and immunostaining*

Uterine tissues were fixed in 10% formalin, embedded in paraffin, and sectioned for hematoxylin and eosin staining according to standard procedures. Immunohistochemistry and immunofluorescence were performed according to previously described methods (Zhang *et al.* 2017; Zhang *et al.* 2016). The endogenous peroxidase and nonspecific binding were removed by incubation with 3% $H_2O_2$ for 10 min and with 10% normal goat serum for 1 h at room temperature. After incubation with the primary antibody (Supplemental Table 1) overnight at 4°C in a humidified chamber, the sections were stained using the avidin-biotinylated-peroxidase complex detection system (Vector Laboratories Inc., Burlingame, CA) followed by treatment with 3-amino-9-ethyl carbazole developing reagent plus High Sensitivity Substrate (SK-4200, Vector Laboratories). The sections were imaged on a Nikon E-1000

microscope (Japan) and photomicrographed using Easy Image 1 (Bergström Instrument AB, Sweden).

The other half of the uterine sections were incubated with primary antibody in 0.01 M Tris-buffered saline supplemented with Triton X-100 (TBST) containing 5% nonfat milk overnight at 4°C, and a secondary antibody was applied at room temperature for 1 h. After the sections were washed with TBST, they were re-suspended in mounting medium containing DAPI (4′,6′-diamidino-2-phenylindole; Vector Laboratories). Sections were examined under an Axiovert 200 confocal microscope (Zeiss, Jena, Germany) equipped with a laser-scanning confocal imaging LSM 710 META system (Carl Zeiss) and photomicrographed. Background settings were adjusted from the examination of negative control specimens. Images of positive staining were adjusted to make optimal use of the dynamic range of detection. The immune staining was quantified by semi-quantitative histogram scoring (Q-H score) as described previously (Mariee *et al.* 2012). All morphological and immunohistochemical assays were performed by at least two researchers in an operator-blinded manner.

***Protein isolation and Western blot analysis***

A detailed explanation of the Western blot analysis protocol has been published (Zhang *et al.* 2017; Zhang *et al.* 2016). Total protein was isolated from whole uterine tissue by homogenization in RIPA buffer (Sigma-Aldrich) supplemented with cOmplete Mini protease inhibitor cocktail tablets (Roche Diagnostics, Mannheim, Germany) and PhosSTOP phosphatase inhibitor cocktail tablets (Roche Diagnostics). After determining total protein by Bradford protein assay, equal amounts (30 μg) of protein were resolved on 4–20% TGX stain-free gels (Bio-Rad Laboratories GmbH, Munich, Germany) and transferred onto PVDF membranes. The membranes were probed with the primary antibody (Supplemental Table 1) in TBST containing 5% non-fat dry milk followed by HRP-conjugated secondary antibody. When necessary, the PVDF membranes were stripped using Restore PLUS Western blot

stripping buffer (Thermo Scientific, Rockford, IL) for 15 minutes at room temperature, washed twice in TBST, and then re-probed. Ultraviolet activation of the Criterion stain-free gel on a ChemiDoc MP Imaging System (Bio-Rad) was used to control for proper loading. Band densitometry was performed using Image Laboratory (Version 5.0, Bio-Rad).

In the present study, we used a novel stain-free technology – ultraviolet activation of the Criterion stain-free gel on a ChemiDoc MP Imaging System (Bio-Rad) – which was used to control proper loading (total protein normalization). This technology represents a significant advancement over existing stain-based total protein quantitation approaches such as Coomassie blue, Ponceau S, and others and gives accurate protein loading control data in a standardized manner without requiring lengthy optimization. The detection of proteins on stain-free gels is based upon trihalocompound modification of tryptophan residues in proteins run on stain-free gels, which are exposed to UV. The modified tryptophans give a fluorescent signal that can be readily detected by a CCD camera. In our study, band densitometry was performed using Image Laboratory. When quantified, the intensity of each protein band was normalized to the total protein in individual sample. This method has been commonly used in both human and animal tissues to semi-quantify concentrations of specific proteins in many studies. Please visit the link given below for review of previous publications using the same method and technology:

(http://www.biorad.com/webroot/web/pdf/lsr/literature/Bulletin_6351.pdf).

***RNA extraction and qRT-PCR analysis***

For RNA isolation, tissues from each rat were lysed using TRIzol Reagent (Life Technologies), and RNA was isolated following standard protocols. qRT-PCR was performed with a Roche Light Cycler 480 sequence detection system (Roche Diagnostics Ltd., Rotkreuz, Switzerland) as previously described (Zhang *et al.* 2017; Zhang *et al.* 2016). The PCR amplifications were performed with a SYBR green qPCR master mix (#K0252, Thermo

Scientific, Rockford, IL). Total RNA was prepared from the frozen whole uterine tissues, and single-stranded cDNA was synthesized from each sample (2 μg) with M-MLV reverse transcriptase (#0000113467, Promega Corporation, Fitchburg, WI) and RNase inhibitor (40 U) (#00314959, Thermo Scientific). cDNA (1 μl) was added to a reaction master mix (10 μl) containing 2× SYBR green qPCR reaction mix (Thermo Scientific) and gene-specific primers (5 μM each of forward and reverse primers). All primers are indicated in Supplemental Table 2. All reactions were performed six times, and each reaction included a non-template control. The results for target genes were expressed as the amount relative to the average CT values of *GAPDH* + *U87* in each sample. Relative gene expression was determined with the $2^{-\Delta\Delta CT}$ method, and the efficiency of each reaction – as determined by linear regression – was incorporated into the equation.

***Measurement of biochemical parameters***

Concentrations of gonadotropins (follicle stimulating hormone and luteinizing hormone), steroid hormones (17β-estradiol, progesterone, testosterone, 5α-dihydrotestosterone, and androstenedione), sex hormone-binding globulin, glucose, and insulin in rat serum samples were measured using commercially available assays (Cloud-Clone Corp., Houston, TX) as described previously (Zhang et al. 2017). All samples and standards were measured in duplicate. The intra- and inter-assay coefficients of variation are listed in Supplemental Table 3.

**References**

Cui P, Li X, Wang X, Feng Y, Lin JF, Billig H & Shao R 2015 Lack of cyclical fluctuations of endometrial GLUT4 expression in women with polycystic ovary syndrome: Evidence for direct regulation of GLUT4 by steroid hormones. *BBA Clinical* **4** 85-91. (https:// doi: 10.1016/j.bbacli.2015.08.004)

Li X, Cui P, Jiang HY, Guo YR, Pishdari B, Hu M, Feng Y, Billig H & Shao R 2015 Reversing the reduced level of endometrial GLUT4 expression in polycystic ovary syndrome:

a mechanistic study of metformin action. *American Journal of Translational Research* **7** 574-586.

Mariee N, Li TC & Laird SM 2012 Expression of leukaemia inhibitory factor and interleukin 15 in endometrium of women with recurrent implantation failure after IVF; correlation with the number of endometrial natural killer cells. *Human Reproduction* **27** 1946-1954. (https://doi: 10.1093/humrep/des134)

Zhang Y, Hu M, Meng F, Sun X, Xu H, Zhang J, Cui P, Morina N, Li X, Li W, et al. 2017 Metformin Ameliorates Uterine Defects in a Rat Model of Polycystic Ovary Syndrome. *EBioMedicine* **18** 157-170. (https://doi: 10.1016/j.ebiom.2017.03.023)

Zhang Y, Sun X, Sun X, Meng F, Hu M, Li X, Li W, Wu XK, Brännström M, Shao R, et al. 2016 Molecular characterization of insulin resistance and glycolytic metabolism in the rat uterus. *Scientific Report* **6** 30679. (https://doi: 10.1038/srep30679)

**Supplementary Table 1.** Antibodies: species, clone/catalog number, method, dilution, and source.

| Antibody | Species | Cat. No. | kDa | Method | Dilution | Source |
|---|---|---|---|---|---|---|
| PGR | Mouse | MA1-410 | B120<br>A94 | WB<br>IHC | 1:500<br>1:50 | Thermo Fisher (Rockford, IL) |
| p-c-Raf | Rabbit | 9427 | 74 | WB | 1:500 | Cell Signaling Technology (Danver, MA) |
| p-MEK1/2 | Rabbit | 9154 | 45 | WB | 1:500 | Cell Signaling Technology |
| p-ERK1/2 | Rabbit | 4370 | 42,44 | WB | 1:1000 | Cell Signaling Technology |
| ERK1/2 | Rabbit | 4695 | 42,44 | WB | 1:2000 | Cell Signaling Technology |
| p-p38 MAPK | Rabbit | 4511 | 43 | WB | 1:300 | Cell Signaling Technology |
| p38 MAPK | Rabbit | 8690 | 40 | WB | 1:1000 | Cell Signaling Technology |
| p-JNK | Rabbit | 4668 | 46,54 | WB | 1:500 | Cell Signaling Technology |
| JNK | Rabbit | 9252 | 46,54 | WB | 1:1000 | Cell Signaling Technology |
| ERα | Mouse | 6F11 | | IHC, IF | 1:50 | Novocastra Laboratories Ltd. (Newcastle upon Tyne, UK) |
| ERβ | Rabbit | Ab3577 | | IF | 1:50 | Abcam (Cambridge, UK) |
| p-histone H3 (Ser10) | Rabbit | 3377 | | IF | 1:100 | Cell Signaling Technology |

PGR, progesterone receptor; p-MEK1/2, phosphorylation-MAP2K1/2; ERK1/2, extracellular signal-regulated kinases 1/2; p38 MAPK, p38 mitogen-activated protein kinase; JNK, jun-amino-terminal kinase; ERα, estrogen receptor alpha; WB, western blot; IHC, immunohistochemistry; IF, immunofluorescence.

**Supplementary Table 2.** Sequences of primer pairs used for qRT-PCR measurement.

| Gene | | Primer | Size |
|---|---|---|---|
| *Ihh* | Forward | CCTCGTAAACTCGTGCCTCT | 222 bp |
| | Reverse | CAGTGAGTTCAGACGGTCCT | |
| *Ptch* | Forward | GAACAAGCAACTTCCCCAAA | 190 bp |
| | Reverse | AATGTCGATGGGCTTGTCTC | |
| *Smo* | Forward | CAATGCGTGTTTCTTTGTGG | 253 bp |
| | Reverse | CGAGAGAGGCTGGTAAGTGG | |
| *Nr2f2* | Forward | GTCGCCTTTATGGACCACAT | 145 bp |
| | Reverse | CGTGGGCTACATCAGACAGA | |
| *Hand2* | Forward | CAGCTACATCGCCTACCTCA | 162 bp |
| | Reverse | TTCTTGTCGTTGCTGCTCAC | |
| *Fkbp5* | Forward | GCTGCCATCGAAAGCTGTAA | 102 bp |
| | Reverse | GTCAAAGTCATTCACGGCCA | |
| *Ncoa2* | Forward | GCGAATGTCACAGAGCACTT | 238 bp |
| | Reverse | ACTGCCAATCATTCCTGTGC | |
| *Pgr* | Forward | GGTCTAAGTCTCTGCCAGGTTTCC | 182 bp |
| | Reverse | CAACTCCTTCATCCTCTGCTCATTC | |
| *Pgrb* | Forward | GCATCGTCTGTAGTCTCGCCAATAC | 176 bp |
| | Reverse | GCTCTGGGATTTCTGCTTCTTCG | |
| *Prl* | Forward | CAAGAAGAAGGGGCCAACCT | 100 bp |
| | Reverse | CTGGTGGTGACTGTCCCTTC | |
| *Igfbp1* | Forward | TGTACTAGAACCTGCCGCAC | 126 bp |
| | Reverse | AGCAGCTGTTCCTCTGTCAT | |
| *Lif* | Forward | CGCCCAACATGACGGATTTC | 226 bp |
| | Reverse | TTGTTGCACAGACGGCAAAG | |
| *Il11* | Forward | GACTCCCTACCTACCTTGGC | 100 bp |
| | Reverse | GCAACCACTGTACATGTCGG | |

| Gene | | Primer | Size |
|---|---|---|---|
| *Pc6* | Forward | GTGTGAGAATGGGTCGGAGA | 149bp |
| | Reverse | TTTCTTTCCACTTTCGGCCG | |
| *Spp1* | Forward | CTGAAGCCTGACCCATCTCA | 143 bp |
| | Reverse | TCGTCGTCATCATCGTCCAT | |
| *Maoa* | Forward | AGGAGCTAGGCATAGAGACCT | 219 bp |
| | Reverse | TCTTGTCCCATTCCTGAGCG | |
| *Ednrb* | Forward | GGGTCTGCATGCTTAATCCC | 212 bp |
| | Reverse | CTTGGCCACTTCTCGTCTCT | |
| *Hoxa10* | Forward | TCCGAAAACAGTAAAGCCTCTC | 127 bp |
| | Reverse | GCGTCTGGTGCTTCGTGTAA | |
| *Hoxa11* | Forward | GACTCCCTACCTACCTTGGC | 100 bp |
| | Reverse | GCAACCACTGTACATGTCGG | |
| *Lrh1* | Forward | CTGTGAAAGCTGCAAGGGTT | 154 bp |
| | Reverse | CAGCTTCATTCCAACGTCGA | |
| *Sgk1* | Forward | GGGCCTTCACTTCTCTTTCC | 163 bp |
| | Reverse | GTGCAGATAACCCAAGGCAC | |
| *Hbegf* | Forward | GCTCTTCCACCTGGCTCAAT | 120 bp |
| | Reverse | CACAACCCACCCTGGGATAC | |
| *Krt13* | Forward | GTTTCGGAGCTGGTTCTTGC | 277 bp |
| | Reverse | AGGCGGTCATTGAGGTTCTG | |
| *Esr1* | Forward | ACGCTCTGCCTTGATCACAC | 132 bp |
| | Reverse | CCTGCTGGTTCAAAAGCGTC | |
| *Esr2* | Forward | AAAGTAGCCGGAAGCTGACA | 138 bp |
| | Reverse | GCCTGACGTGAGAAAGAAGC | |
| *Gapdh* | Forward | TCTCTGCTCCTCCCTGTTCTA | 121 bp |
| | Reverse | GGTAACCAGGCGTCCGATAC | |
| *U87* | Forward | CCAGGTGCAACAAAACCTGT | 188 bp |
| | Reverse | GCTGGACCCAAAACAACGAG | |

*Pgr*, progesterone receptor; *Ihh*, Indian hedgehog; *Ptch*, patched; *Smo*, smoothened frizzled class receptor; *Nr2f2*, nuclear receptor subfamily 2 group F member 2; *Hand2*, heart and neural crest derivatives expressed 2; *Fkbp5*, FK506 binding protein 5; *Ncoa2*, nuclear receptor coactivator 2; *Pgr*, progesterone receptor; *Pgrb*, progesterone receptor B; *Prl*, prolactin; *Igfbp1*, insulin-like growth factor binding protein 1; *Lif*, leukemia inhibitory factor; *Pc6*, subtilisin/kexin type 6; *Spp1*, osteopontin/secreted phosphoprotein 1; *Maoa*, monoamine oxidase; *Ednrb*, endothelin receptor B; *Hoxa10*, homeobox A10; *Lrh1*, liver receptor homolog-1; *Sgk1*, serum- and glucocorticoid-regulated kinase; *Hbegf*, heparin-binding EGF-like growth factor; *Krt13*, keratin 13; *Esr1*, estrogen receptor 1; *Gapdh*, glyceraldehyde-3-phosphate dehydrogenase; *U87*, small nucleolar RNA, C/D box 87(Snord87).

**Supplementary Table 3.** The intra-assay and inter-assay % CV for the rat gonadotropins, steroid hormones, and insulin.

| | **Intra-assay % CV** | **Inter-assay % CV** |
|---|---|---|
| FSH | 6.4 | 6.8 |
| LH | 6.4 | 6.6 |
| E2 | 6.5 | 6.8 |
| P4 | 6.4 | 6.6 |
| Total T | 6.2 | 6.6 |
| A4 | 6.7 | 6.9 |
| DHT | 6.2 | 6.7 |
| SHBG | 6.4 | 6.8 |
| Insulin | 6.3 | 6.6 |

FSH, follicle-stimulating hormone; LH, luteinizing hormone; E2, 17β-estradiol; P4, progesterone; T, testosterone; A4, androstenedione; DHT, 5α-dihydrotestosterone; SHBG, sex hormone-binding globulin.

**Supplementary Table 4.** Effects of implantation on the endocrine and metabolic alterations in control rats treated with saline or metformin, and insulin+hCG-treated (PCOS-like) rats with metformin.

| | **Saline** (n = 8) | **Met** (n = 10) | **Insulin + hCG + Met (implantation)** (n = 10) | **Insulin + hCG + Met (no implantation)** (n = 5) |
|---|---|---|---|---|
| FSH (ng/ml) | 2.13 ± 0.04 | 2.06 ± 0.04 | 2.14 ± 0.04 | 2.14 ± 0.10 |
| LH (ng/ml) | 2.00 ± 0.24 | 1.93 ± 0.11 | 2.31 ± 0.17 | 2.73 ± 0.36 |
| LH / FSH | 0.94 ± 0.11 | 0.94 ± 0.05 | 1.08 ± 0.08 | 1.28 ± 0.18 |
| E2 (ng/ml) | 1.31 ± 0.04 | 1.34 ± 0.03 | 1.23 ± 0.03 | 1.32 ± 0.05 |
| P4 (ng/ml) | 6.88 ± 0.35 | 6.51 ± 0.37 | 8.95 ± 0.44 [a, c] | 4.80 ± 0.11 [b, d, e] |
| Total T (ng/ml) | 5.11 ± 0.71 | 3.83 ± 0.22 | 3.78 ± 0.44 | 7.40 ± 0.09 [a, c, e] |
| A4 (ng/ml) | 0.142 ± 0.004 | 0.142 ± 0.006 | 0.162 ± 0.006 | 0.181 ± 0.016 [b, c] |
| DHT (pg/ml) | 102.97 ± 5.66 | 97.92 ± 9.28 | 102.00 ± 5.52 | 154.58 ± 8.39 [a, c, e] |
| E2 / Total T | 0.29 ± 0.04 | 0.36 ± 0.02 | 0.38 ± 0.05 | 0.18 ± 0.01 [d, f] |
| Total T / DHT | 0.051± 0.007 | 0.044 ± 0.006 | 0.038 ± 0.005 | 0.049 ± 0.003 |
| Total T / A4 | 36.37 ± 5.36 | 27.28 ± 1.77 | 23.26 ± 2.49 | 42.20 ± 3.52 [d, e] |
| SHBG (ng/ml) | 11.08 ± 0.33 | 10.89 ± 0.35 | 9.67 ± 1.16 | 10.91 ± 0.56 |
| Fasting glucose (mmol/l) | 4.19 ± 0.09 | 3.92 ± 0.10 | 4.53 ± 0.19 [d] | 4.98 ± 0.12 [a, c] |
| Fasting insulin (pg/ml) | 3.26 ± 0.05 | 3.17 ± 0.02 | 3.22 ± 0.04 | 3.42 ± 0.03 [b, c, f] |
| HOMA-IR | 0.61 ± 0.01 | 0.55 ± 0.01 | 0.65 ± 0.03 [c] | 0.76 ± 0.02 [a, c, f] |

Met, metformin; FSH, follicle-stimulating hormone; LH, luteinizing hormone; E2, 17α-estradiol; P4, progesterone; T, testosterone; A4, androstenedione; DHT, 5α-dihydrotestosterone; SHBG, sex hormone-binding globulin; HOMA-IR, Homeostasis model assessment of insulin resistance, HOMA-IR= fasting blood glucose (mmol/l) × fasting serum insulin (μU/ml) / 22.5.

Values are Mean ±SEM. The multiple comparisons between data were performed using one-way ANOVA and Tukey's post hoc test. A P-value less than 0.05 was considered statistically significant.

[a] $P < 0.01$ versus Saline group.

[b] $P < 0.05$ versus Saline group.

[c] $P < 0.01$ versus Met group.

[d] $P < 0.05$ versus Met group.

[e] $P < 0.01$ versus Insulin + hCG + Met (implantation) group.

[f] $P < 0.05$ versus Insulin + hCG + Met (implantation) group.

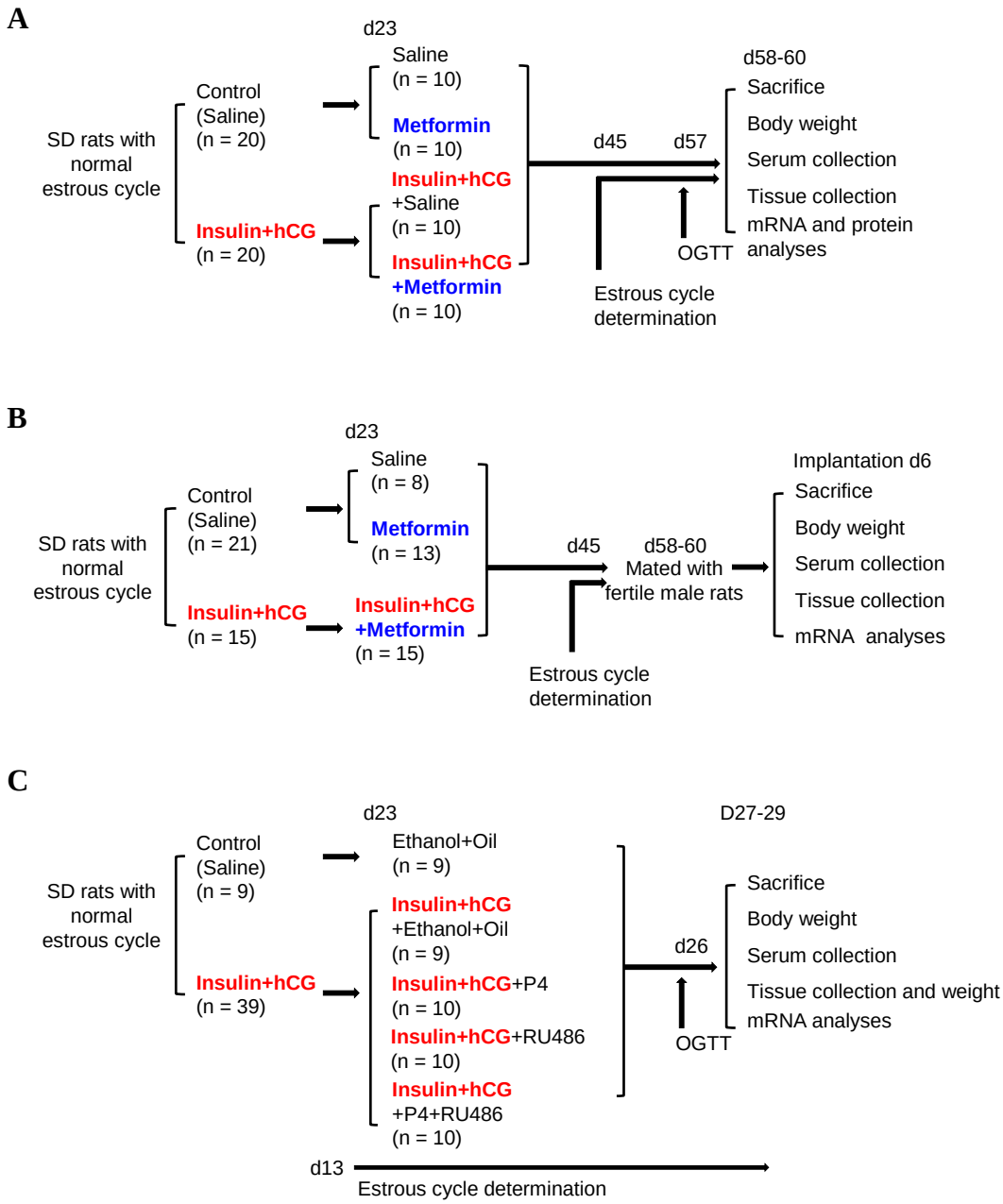
A
d23
Saline
(n = 10)
Metformin
(n = 10)
Insulin+hCG
+Saline
(n = 10)
Insulin+hCG
+Metformin
(n = 10)
SD rats with
normal
estrous cycle
Control
(Saline)
(n = 20)
Insulin+hCG
(n = 20)
d45
d57
d58-60
Sacrifice
Body weight
Serum collection
Tissue collection
mRNA and protein
analyses
OGTT
Estrous cycle
determination
B
d23
Saline
(n = 8)
Metformin
(n = 13)
Insulin+hCG
+Metformin
(n = 15)
SD rats with
normal
estrous cycle
Control
(Saline)
(n = 21)
Insulin+hCG
(n = 15)
d45
d58-60
Mated with
fertile male rats
Implantation d6
Sacrifice
Body weight
Serum collection
Tissue collection
mRNA analyses
Estrous cycle
determination
C
d23
Ethanol+Oil
(n = 9)
Insulin+hCG
+Ethanol+Oil
(n = 9)
Insulin+hCG+P4
(n = 10)
Insulin+hCG+RU486
(n = 10)
Insulin+hCG
+P4+RU486
(n = 10)
SD rats with
normal
estrous cycle
Control
(Saline)
(n = 9)
Insulin+hCG
(n = 39)
d26
D27-29
Sacrifice
Body weight
Serum collection
Tissue collection and weight
mRNA analyses
OGTT
d13
Estrous cycle determination

# Suppl Figure 2

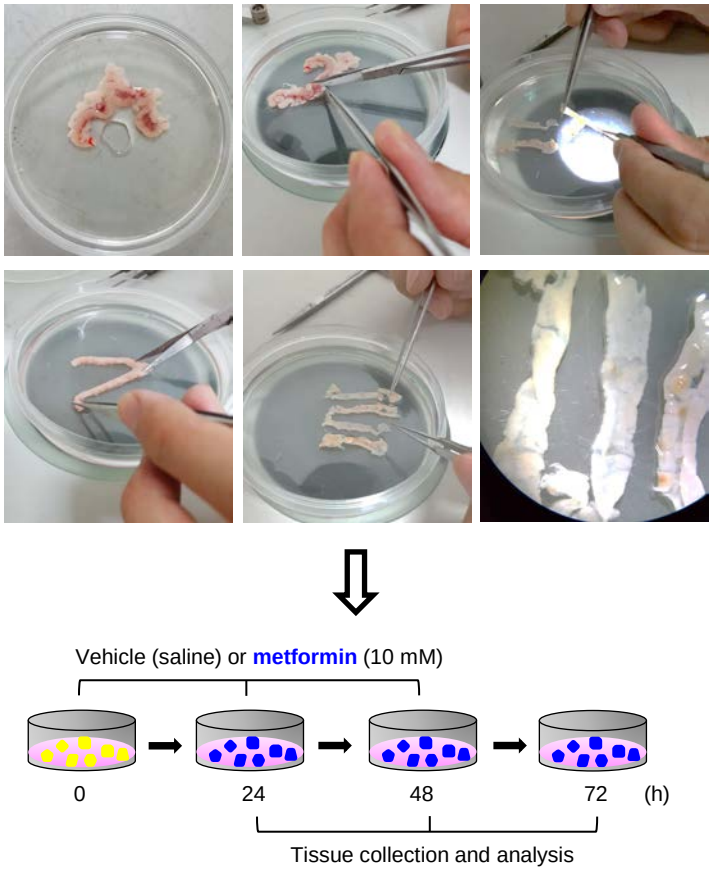

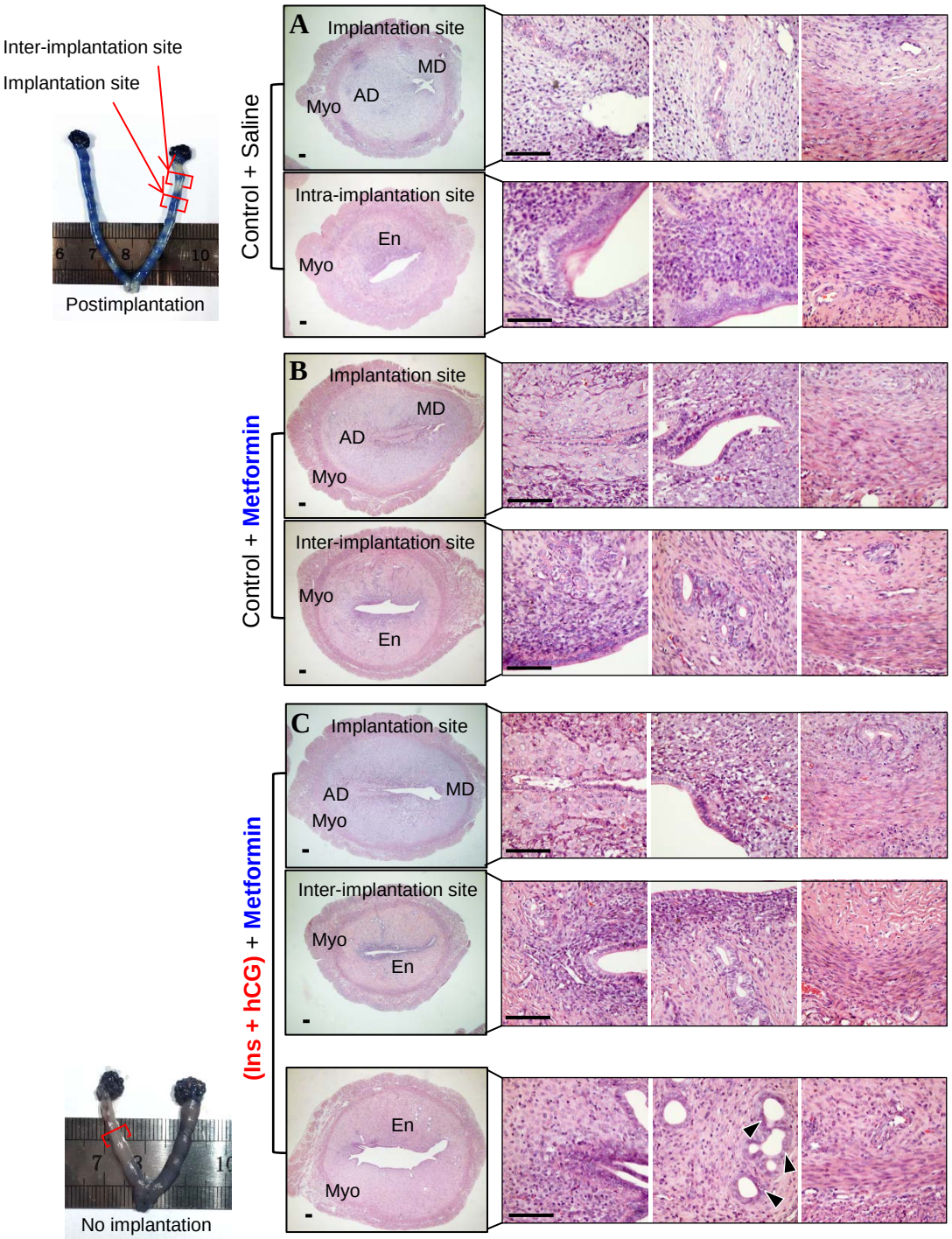
Inter-implantation site
Implantation site
Postimplantation
Control + Saline
A
Implantation site
MD
AD
Myo
Intra-implantation site
En
Myo
Control + Metformin
B
Implantation site
MD
AD
Myo
Inter-implantation site
Myo
En
(Ins + hCG) + Metformin
C
Implantation site
AD
MD
Myo
Inter-implantation site
Myo
En
En
Myo
No implantation

# Suppl Figure 4

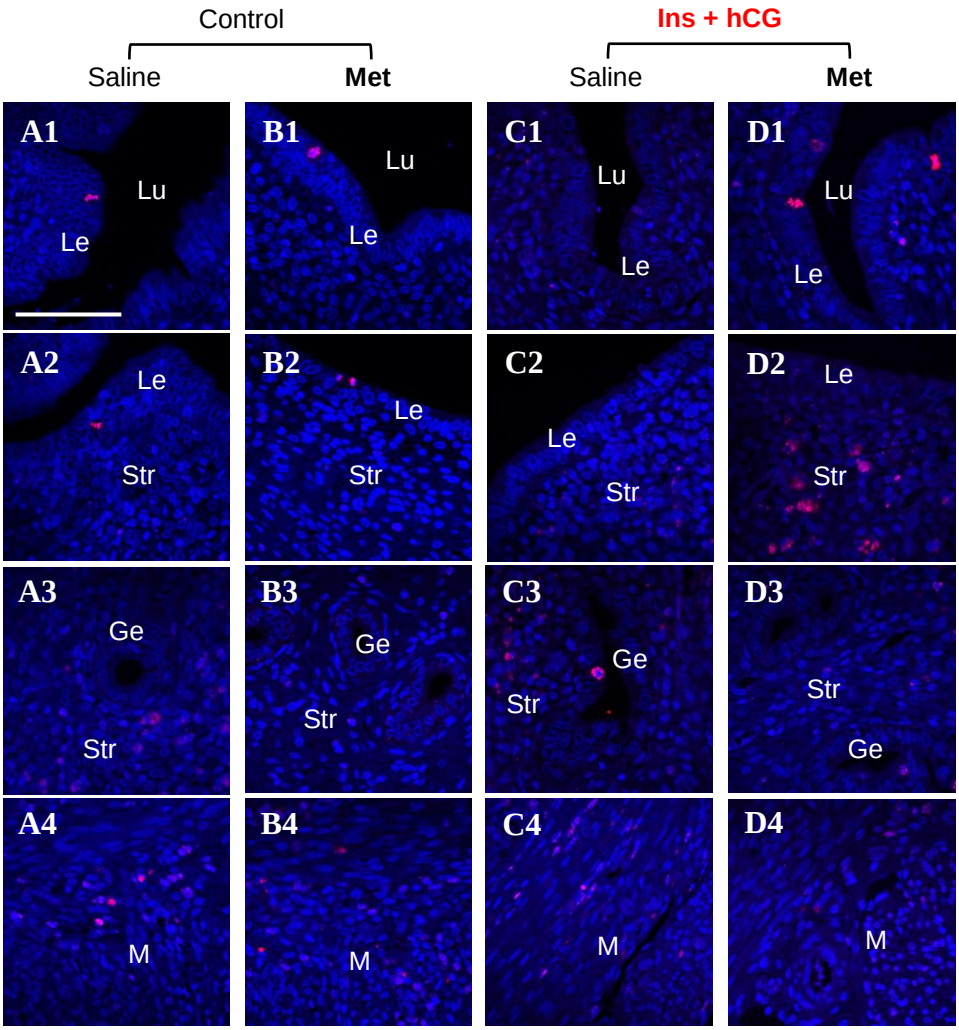


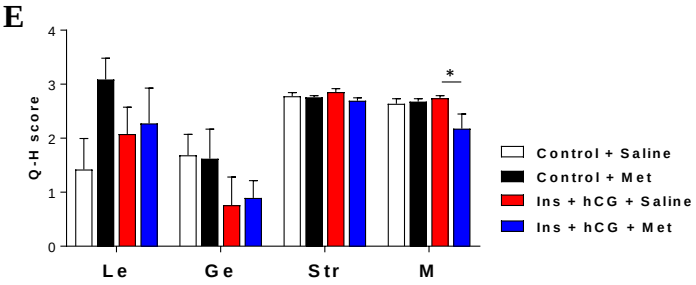

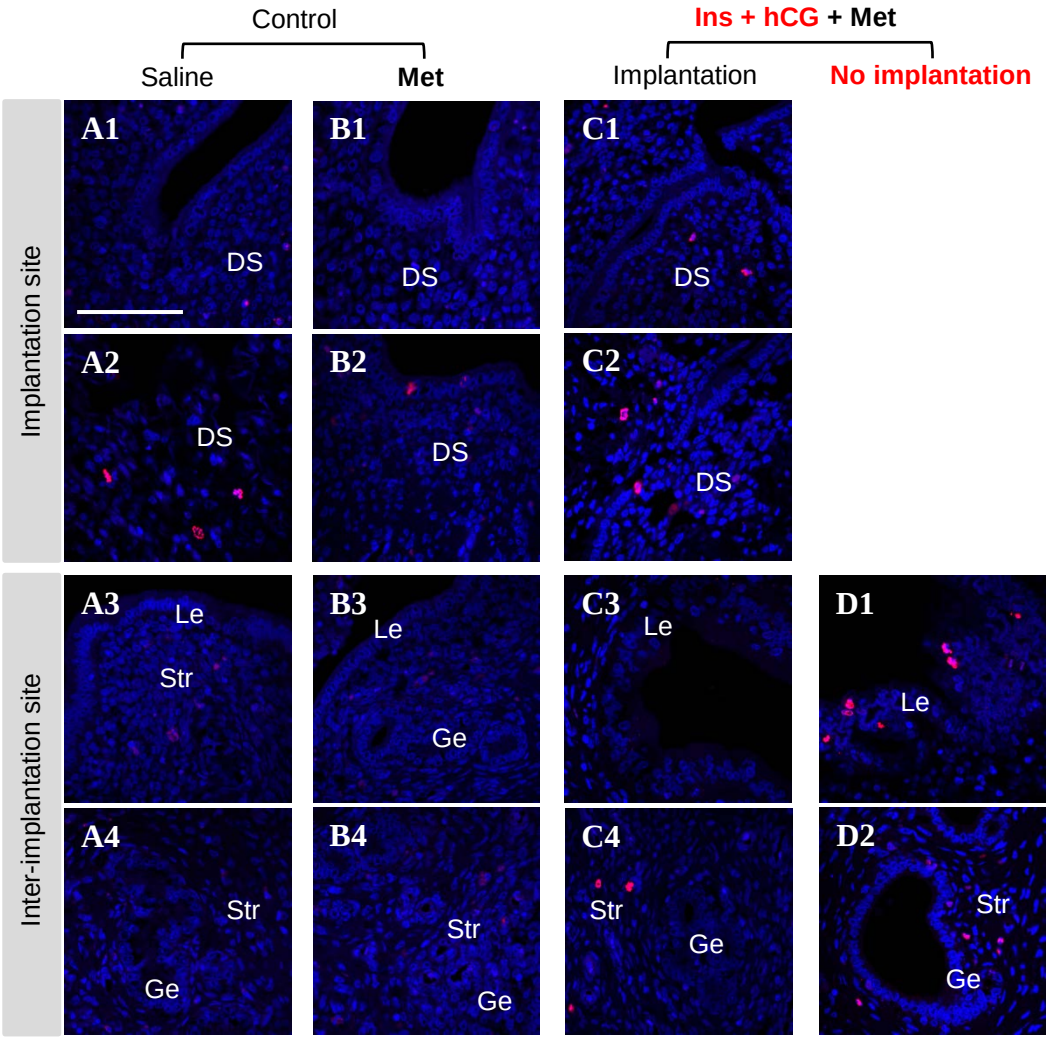
Control
Ins + hCG + Met
Saline
Met
Implantation
No implantation
Implantation site
Inter-implantation site
A1
B1
C1
A2
B2
C2
A3
B3
C3
D1
A4
B4
C4
D2
DS
Le
Str
Ge

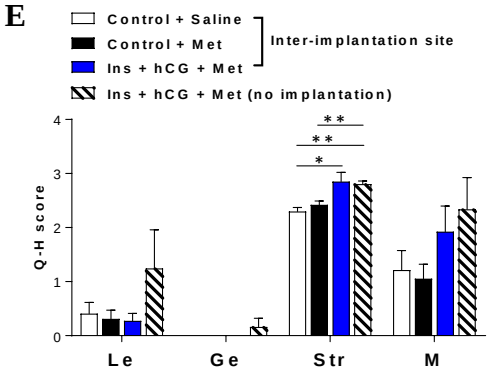
E
Control + Saline
Control + Met
Ins + hCG + Met
Inter-implantation site
Ins + hCG + Met (no implantation)
Q-H score
0
1
2
3
4
**
**
*
Le
Ge
Str
M